



PATS#424110

Comprehensive Multidimensional GC and Pyrolysis-GC/MS for the Analysis of Integrated Circuit Package Materials

GCxGC/MS Method Development for Qualitative Analysis of VOCs in Die Attach Adhesives and Pyrolysis-GC/MS Method Development for Fingerprinting and Material Characterization of Epoxy Molding Compounds

Bachelor thesis, June 2022

T.H. Scholten

Chemistry (HLO) student at HAN University of Applied Sciences
Graduate intern analytical chemistry at NXP Semiconductors, Nijmegen

under supervision of

L. Goumans

Material & Process Engineer at NXP Semiconductors Netherlands B.V.

M.H.M. van der Straaten

Principal Engineer Physical Analysis at NXP Semiconductors Netherlands B.V.

Academic supervisor: J. Kraan MEd

Major: Analytical Chemistry

Student number: 616988



Acknowledgements

My graduation internship at NXP semiconductors has been a very valuable experience for me. I have been able to expand my expertise in the field of analytical chemistry and gained further experience with working in a professional environment. I want to thank Leon Goumans for supervising me during this period. His exceptional positivity and helpful instructions have been very important for me. I also want to thank Marcel van der Straaten for taking the role as supervisor when Leon was not available. His feedback and instructions during the writing of this thesis have been very helpful. Lastly, I want to thank my academic supervisor Jeroen Kraan for his guidance during my graduation internship. I appreciate that he was always willing to provide support when needed.



List of abbreviations

CIS	Cooled Injection System
DAA	Die Attach Adhesive
DoE	Design of Experiment
D_f	Film thickness
EGA	Evolved Gas Analysis
EMC	Epoxy Molding Compound
FID	Flame Ionization Detector
GC	Gas Chromatography
GCxGC	Comprehensive multidimensional gas chromatography
IC	Integrated Circuit
I.D.	Inner Diameter
MS	Mass Spectrometry/Mass Spectrometer
PCM	Pneumatic Control Module
PYR	Pyrolysis
RSD	Relative Standard Deviation
SD	Standard Deviation
TD	Thermal Desorption
TDU	Thermal Desorption Unit
TGA	Thermogravimetric Analysis
VOC	Volatile Organic Compound

Summary

Both consumer and industrial electronics have become increasingly complex and advanced in recent years. High performance semiconductor devices are essential to the function of these electronics, which is why rapid growth of the microelectronics industry and major technological advancements in this field have been necessary to meet demands. NXP semiconductors contributes to these technological developments by designing and manufacturing semiconductor devices for application in, for example, the automotive- and mobile industry. The Product Diagnostics Centre at NXP plays a critical role in assuring that high quality products are manufactured by carrying out electrical-, physical- and chemical analyses. Comprehensive multidimensional GC (GCxGC) and pyrolysis have been introduced at NXP semiconductors to enhance the quality and extent of the analyses of integrated circuit (IC) package materials. Method development for GCxGC/MS and Pyrolysis – Gas Chromatography/Mass Spectrometry (PYR-GC/MS), and subsequent evaluation of the capabilities of both techniques were therefore carried out in two separate projects.

The goal concerning GCxGC/MS consisted of two parts. First, a method had to be developed in which GCxGC parameter settings were optimized to maximize both separation and detection of volatile organic compounds (VOCs) in die attach adhesives (DAAs). After that, the additional value of GCxGC analysis compared to the traditionally applied single column GC analysis had to be assessed with regard to compound separation and compound identification. GCxGC parameters settings for 1D flow rate, 2D flow rate and oven temperature ramp were optimized by Experimental Design, maximizing 1D resolution, 2D resolution and peak area. A 1D flow rate of 0.525 mL/min, 2D flow rate of 20 mL/min and an oven temperature ramp of 4.5°C/min were selected as parameter settings for the general GCxGC/MS method.

The additional value of GCxGC compared to single column GC was assessed by considering compound separation, reliability of compound identification and repeatability of peak area. GCxGC/MS analysis of VOCs in DAA resulted in compound separation that could not be achieved by single column GC/MS analysis, which illustrated the additional value of GCxGC for this purpose. However, the repeatability of peak area was poor and compound identification results turned out to be largely unreliable as well. It was therefore concluded that the current application of GCxGC/MS at NXP provides additional value compared to the current single column GC/MS analysis with regard to compound separation, but may need further optimization when it comes to repeatability and compound identification.

The goal concerning PYR-GC/MS was to create a method that can generate fingerprints of epoxy molding compounds (EMCs), and would allow for an initial exploration of the capabilities of PYR-GC/MS with regard to material characterization. Pyrolysis temperatures for both pulsed- and smart ramp pyrolysis were determined based on the data of evolved gas analysis. Temperatures of 425°C and 575°C were selected for pulsed PYR-GC/MS, and 625°C was selected as end temperature for smart ramp pyrolysis. A pyrolysis duration of 12 seconds was selected for both pulsed and smart ramp pyrolysis.

Pulsed PYR-GC/MS analysis of EMCs resulted in characteristic chromatograms with excellent repeatability. The developed pulsed PYR-GC/MS method can therefore be used to generate EMC fingerprints. The application of the method regarding material characterization was also explored. The compounds that were identified after analysis of EMCs indicated that pulsed PYR-GC/MS analysis can be used to gain insight into the composition of EMCs. The application of smart ramp PYR-GC/MS showed promising results for this purpose as well.



Table of contents

1. Introduction.....	6
2. Theoretical background.....	8
2.1 IC packages	8
2.1.1 Die attach adhesives.....	8
2.1.2 Epoxy molding compounds.....	9
2.2 Gas chromatography.....	10
2.2.1 Comprehensive Multidimensional GC (GCxGC).....	10
2.2.2 Modulators	11
2.2.3 Flow rate compatibility and GCxGC operating window	12
2.2.4 GCxGC columns	14
2.3 Thermal desorption.....	16
2.4 Pyrolysis.....	16
2.5 Thermogravimetric analysis by evolved gas analysis.....	17
3. Experimental.....	19
3.1 Chemicals and materials.....	19
3.2 Instruments, equipment and software.....	19
3.3 GCxGC/MS method development and application	20
3.3.1 Determination of GCxGC operating window.....	20
3.3.2 Determination of DoE factor ranges.....	21
3.3.3 Execution of DoE and selection of optimal settings	21
3.3.4 Assessment of repeatability	22
3.3.5 Single column GC versus GCxGC.....	22
3.4 Pyrolysis-GC/MS method development and application	23
3.4.1 Pyrolysis temperatures from evolved gas analysis	23
3.4.2 Selection of pyrolysis duration and application of PYR-GC/MS.....	24
4. Results.....	25
4.1 GCxGC/MS method development and application	25
4.1.1 GCxGC operating window	25
4.1.2 DoE factor ranges	27



4.1.3 DoE and selection of optimal settings	28
4.1.4 Repeatability of peak area	32
4.1.5 Single column GC vs GCxGC	33
4.2 PYR-GC/MS method development	35
4.2.1 Pyrolysis temperatures from evolved gas analysis	35
4.2.2 Selection of initial times.....	36
4.2.3 Pulsed PYR-GC/MS for EMC fingerprinting	36
4.2.4 PYR-GC/MS for material characterization	38
5. Discussion.....	40
5.1 GCxGC/MS	40
5.2 PYR-GC/MS	42
6. Conclusions.....	44
6.1 GCxGC/MS	44
6.2 PYR-GC/MS	44
7. Bibliography.....	46
8. Appendices	48

1. Introduction

Microelectronic semiconductor devices such as integrated circuits (ICs) are essential to the function of for example, electric vehicles, mobile phones, industrial equipment and wireless infrastructure. The complexity and functionality of applications such as these have increased rapidly during the last decade, thanks to major technological advancements. This has created an ever-growing demand for high performance and innovative semiconductor devices to ensure proper functionality and secure connectivity. NXP Semiconductors designs and manufactures a wide variety of such devices to contribute to the development of a smarter and more connected world. The devices find specific applications in NXP's business lines Automotive, Mobile, Industrial, Wireless infrastructure, Smart city and Smart home (NXP Semiconductors, 2022).

NXP aims to develop and manufacture high quality products and provide high quality customer service. Diagnostic centers contribute to these purposes through failure analyses, process- and material analyses, board level reliability tests, problem solving and problem preventing. The Product Diagnostics Centre at NXP Nijmegen carries out electrical, physical and chemical analyses, for which a wide range of techniques are used. For chemical analysis, these include FTIR, ICP-OES, ICP-MS, IC-MS, GC/MS and HPLC.

GC/MS has traditionally been used at NXP for qualitative and quantitative analysis of volatile organic compounds (VOCs) in die attach adhesives (DAAs). DAAs are used to secure an IC die to the package or substrate. Most uncured DAAs are epoxy- or acrylate-based materials, mixed with fillers and curing agents (Gotro, 2017). GC/MS data provides information about the composition of DAAs in terms of VOCs, including environmentally hazardous compounds. The newly installed GC/MS system at NXP has comprehensive multidimensional GC (GCxGC) and pyrolysis as two additional features to the older GC/MS system. Two techniques that had not been applied before at NXP. NXP aims to explore the capabilities of GCxGC and pyrolysis by developing methods for both techniques to enhance the quality and extent of material analysis. Applications of GCxGC and pyrolysis were therefore studied in two separate projects, of which the findings are presented in this thesis.

GCxGC is a powerful separation technique utilizing two columns of differing phase selectivity in series. It can provide improved peak capacity, better separation and higher sensitivity compared to single column GC, which can lead to more reliable compound identification (LECO Empowering Results, n.d.). Its application may prove to be beneficial for NXP in the qualitative analysis of VOCs in various materials, such as DAAs. The analysis of these VOCs is currently carried out by single column GC/MS and results in compromised identification, possibly due to coelution. The potential additional value of GCxGC compared to single column GC with regard to compound separation and compound identification was therefore studied by developing and subsequently applying a GCxGC/MS method for the qualitative analysis of VOCs in DAAs.

The goals concerning GCxGC were to first develop a method in which GCxGC parameter settings were optimized to maximize both separation and detection of VOCs in DAAs, and then assess the additional value of GCxGC analysis compared to the traditionally applied single column GC analysis with regard to compound separation and compound identification.

GCxGC/MS method development was carried out by optimizing 1D flow rate, 2D flow rate and oven temperature ramp to maximize 1D resolution, 2D resolution and peak area. The optimal 1D- and 2D flow rates were expected to fall within the range of 0.4 – 0.65 mL/min and 15 – 27.5 mL/min (Gestel, W. van., GCxGC training Da Vinci, Feb 16, 2022). The optimal oven temperature ramp was expected to fall within the range of 3 – 6°C (Gestel, W. van., GCxGC training Da Vinci, Feb 16, 2022), (Griffith et al., 2012), (Mostafa et al., 2012). GCxGC/MS method development was carried out by first determining which 1D- and 2D flow rates are compatible, to avoid undesirable chromatographic effects. Parameter settings for 1D flow rate, 2D flow rate and oven temperature ramp were then optimized by means of Experimental Design in which 1D resolution, 2D resolution and peak area served as responses. The additional value of GCxGC compared to single column GC was assessed by considering compound separation, compound identification. Repeatability of peak area was determined as well, to assess the reliability of GCxGC/MS results in that respect. It was expected that GCxGC/MS analysis would result in both improved separation and improved compound identification (Liu, J., 2018), (Mostafa et al., 2012), (Ong & Marriott, 2002), (Shimadzu, 2012), (Winnike et al., 2015).

The pyrolysis option on the new GC/MS facilitates complete decomposition of liquid and solid samples under inert conditions. The technique is mainly used for the characterization of macro molecules, such as polymers. Research has shown that PYR-GC/MS analysis at optimal temperatures results in the detection of characteristic fragments, called pyrolysates. PYR-GC/MS is therefore used to generate fingerprints of materials, because the complex mixture of pyrolysates resulting from pyrolysis is unique for each type of material. It can also be used for material characterization, because the characteristic pyrolysates can in principle be traced back to the original sample (Kleine Benne, E. & Zhou, H. X., Gerstel GmbH & Co. KG, video lecture on pyrolysis), (Kusch, 2017), (Rial-Otero et al., 2009).

It was for these reasons that the application of pyrolysis was expected to be of value for NXP in the analysis of epoxy molding compounds (EMCs). EMCs are used at NXP to encapsulate electronic devices for protection against physical stress, heat and moisture. They are complex formulations of fillers, epoxy resins, catalysts, releasing agents, pigments, flame retardants and various performance promoting additives (Procter, n.d.). PYR-GC/MS analysis of these EMC formulations was expected to result in complex chromatograms that can serve as fingerprints and can provide insight into the composition of the material.

The goal concerning the pyrolysis option was to create a PYR-GC/MS method that can generate EMC fingerprints and would allow for an initial exploration of the capabilities of PYR-GC/MS with regard to material characterization. PYR-GC/MS was studied in pulsed and smart ramp mode.

Initial temperatures and an initial time were selected for pulsed PYR-GC/MS to enable the generation of fingerprints and to explore the possibilities of material characterization of EMCs. An end temperature and initial time for smart ramp pyrolysis were selected to enable a comparison between pulsed- and smart ramp pyrolysis regarding their application for material characterization. The optimal initial temperature(s) and end temperature were expected to be dependent on the decomposition temperatures of the EMCs (Ma et al., 2014). Thermogravimetric analysis was therefore simulated by evolved gas analysis to identify the main decomposition temperatures. The required initial time(s) were to be at least 10 seconds (Kleine Benne, E. & Zhou, H. X., Gerstel GmbH & Co. KG, video lecture on pyrolysis). The significance of the pyrolysis duration was investigated by applying three different initial times above 10 seconds.

2. Theoretical background

Analytical methods for GCxGC/MS and PYR-GC/MS have been developed during two separate projects. A GCxGC/MS method has been developed for the qualitative analysis of VOCs in DAAs, and a PYR-GC/MS method has been developed for fingerprinting and material characterization of EMCs. Theoretical background on the composition and application of EMCs and DAAs in IC-packages is provided below, followed by an explanation of the principles of GCxGC and pyrolysis. Other techniques and processes involved during method development, such as thermal desorption and evolved gas analysis, are discussed as well.

2.1 IC packages

IC packages come in a variety of form factors and are specifically designed to suit their application. In their most basic form, IC packages consist of a chip (die), which is glued to a copper die pad with die attach adhesive (DAA) and bonded to copper leads by gold wires. The electronic package is encapsulated by epoxy molding compound (EMC), as illustrated in figure 1.

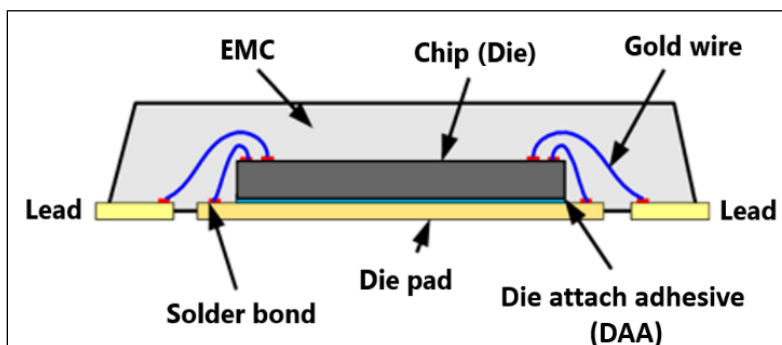


Figure 1: Schematic cross section of a basic IC package including the names of its parts (Lai & Ho, 2004).

2.1.1 Die attach adhesives

Die attach adhesives (DAAs) are used to secure the die to the die pad in an IC package (figure 1). DAAs can either be applied to the die in paste or film form. The DAAs for which a GCxGC/MS method has been developed fall within the paste category. Paste DAAs are mostly epoxy-based, but they can also be acrylate-based. The epoxies and acrylates are present in uncured DAAs as monomers and oligomers. This ensures that the viscosity is low and that it can be easily dispensed on the die through a syringe (Gotro, 2017).

DAAs can vary in electrical and thermal conductivity, depending on the requirements for the package. Desired electrical and thermal conductivity can be achieved by using the correct fillers. Examples of filler types are silver, copper, gold, silica and Teflon. These fillers also help to achieve the right properties in terms of rheology and thermal expansion (Gotro, 2017). The exact composition of the DAAs used at NXP is only known to the supplier. The additional value of GCxGC for the qualitative analysis of VOCs in DAAs was for that reason investigated.

2.1.2 Epoxy molding compounds

Encapsulation of the electronic package by EMC protects the electronic components against physical stress, heat and moisture (Sumitomo Bakelite Co., Ltd., 2015). EMCs contain several raw materials such as filler, epoxy resin, hardener, flame retardant, catalyst and releasing agent. Examples of these raw materials are listed in table 1. Examples of resins added to the molding compound are Epoxy cresol Novolac (ECN), dicyclopentadiene Novolac type epoxy, multi-functional type epoxy, multi aromatic epoxy resins (MAR) and bi-phenyl type epoxy (figure 2) (Fan, 2015) (Sasajima et al., 2016).

Table 1: Overview of materials commonly present in epoxy molding compounds with examples and % Weight (Fan, 2015) (Sasajima et al., 2016).

Raw materials	Examples	% Weight
Filler	Fused silica SiO ₂	80-90
Resin	Epoxy cresol Novolac (ECN), dicyclopentadiene Novolac type epoxy, multi-functional type epoxy, multi aromatic epoxy resins (MAR), bi-phenyl type epoxy	5-10
Hardener	Phenol Novolac, Flexible phenol	5-10
Flame retardant	Brominated Epoxy, Sb ₂ O ₃ , Magnesium hydroxide,	<10
Catalyst	Phosphine	<1
Coupling agent	Epoxy silane, Amino Silane	<1
Releasing agent	Natural Wax, Synthetic wax	<1
Others	Carbon black colorant Rubber like additives as low stress additives	<1

The EMCs used during PYR-GC/MS method development were known to contain multi aromatic resins, and in one case Epoxy cresol Novolac resins. The complete composition of the EMCs is only known to the supplier and only the material properties are shared with NXP. Identification of raw materials as listed in table 1 is therefore in the interest of NXP, which is why the application of PYR-GC/MS for material characterization was considered. EMC fingerprinting by PYR-GC/MS could prove to be useful for quality control of EMC composition.

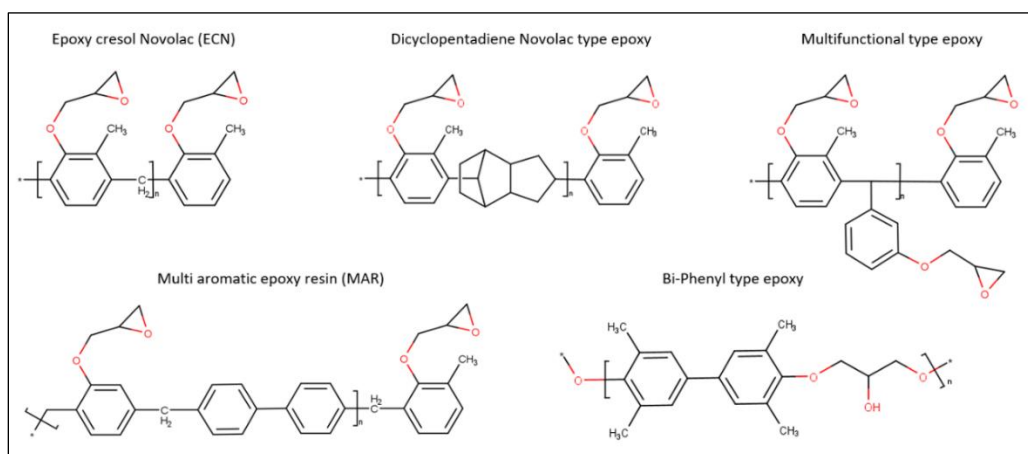


Figure 2: Structural formulas of epoxidized cresol Novolac (ECN), dicyclopentadiene type Novolac epoxy, multi-functional type epoxy, multi aromatic resin (MAR) and biphenyl type epoxy (Sasajima et al., 2016) (Own work).

2.2 Gas chromatography

Chromatography is one of the most widely used techniques for the separation and quantification of components in mixtures. Gas chromatography (GC) is the method of choice for this purpose when it comes to analysis of volatile and semi-volatile compounds. The separation of a gaseous mixture of components is achieved over a column through which a carrier gas (mobile phase) flows. GC-columns come in packed and open tubular forms and contain a polymeric stationary phase which is chemically bonded to an underlying surface of fused silica. Separation of the analytes takes place based on differences in partitioning of the analytes between the stationary phase and the mobile phase (Harris, 2016).

Single column GC has traditionally been applied at NXP for the analysis of VOCs in and DAAs. Method development for qualitative GCxGC/MS analysis of VOCs in DAAs was carried out to determine the additional value of GCxGC compared to single column GC with regard to compound separation and compound identification.

2.2.1 Comprehensive Multidimensional GC (GCxGC)

Comprehensive multidimensional gas chromatography (GCxGC) is a form of 2D GC. It distinguishes itself from 2D heart cutting GC in that the entire sample is analyzed in two dimensions instead of only a portion (heart cut). GCxGC is commonly used for the analysis of complex mixtures such as environmental, biological and petrochemical samples, and can provide improved peak separation and peak capacity compared to single column GC (Agilent Technologies, Inc., 2007).

A GCxGC set-up usually consists of a long, non-polar primary column coupled to a short, polar secondary column. Dimensions such as column length, inner diameter (I.D) and film thickness (D_f) vary depending on the application (Mostafa et al., 2012). The non-polar primary column separates mainly based on dispersive forces, causing some components with different polarities, but equal boiling point, to coelute. The separation of these coeluting components is then enhanced by the secondary column, where the components are mainly separated based on polarity (Shimadzu, 2012). The resulting GCxGC chromatogram can be depicted as a 3D image with the first dimension RT on the x-axis, the second dimension RT on the y-axis and peak intensities on the z-axis (Ong & Marriott, 2002).

The column configuration applied during the project concerning GCxGC/MS method development is illustrated in figure 3. Its operation is as follows: a gaseous sample is introduced through the inlet into the primary column. Effluent from the primary column is then periodically reinjected into the secondary column. The secondary column is connected to a three-way splitter, which directs the effluent from the secondary column to both an FID and an MS detector through short, deactivated transfer lines. The split ratio is dependent on the oven temperature and varies between approximately 1:8 and 1:5 in favor of the FID. Splitting of flow to the detectors is necessary due to the high flow rate of around 20 mL/min in the second dimension. The acquisition rate of the single quadrupole MS that was used is too low for such a flow rate (Shimadzu, 2012). A relatively low flow rate of between 0.4-0.65 mL/min is applied in the primary column to make sure that the 1D and 2D flow rates are compatible with each other. This concept of flow rate compatibility is further explained in paragraph 2.2.3.

A slow oven temperature ramp of around 3-6°C/min is applied to broaden the peaks in the first dimension. This is done to make sure that each 1D peak can be cut in a sufficient amount of fractions. A minimal of three 2D separations per 1D peak is required to preserve the separation achieved in the first dimension

(Mostafa et al., 2012), (Shimadzu, 2012). An oven temperature ramp higher than 6°C/min is likely to cause non-isothermal modulation of a peak, which would result in a drift in 2D retention time within a peak. (Gestel, W. van., GCxGC training Da Vinci, Feb 16, 2022). The periodic reinjection of effluent from the primary column into the secondary column is regulated by the modulator. Carrier gas flow through the modulator is regulated by a pneumatic control module (PCM), and a deactivated restriction column is coupled to the modulator to vent excess gas. The modulator is commonly regarded as the ‘heart’ of the GCxGC configuration.

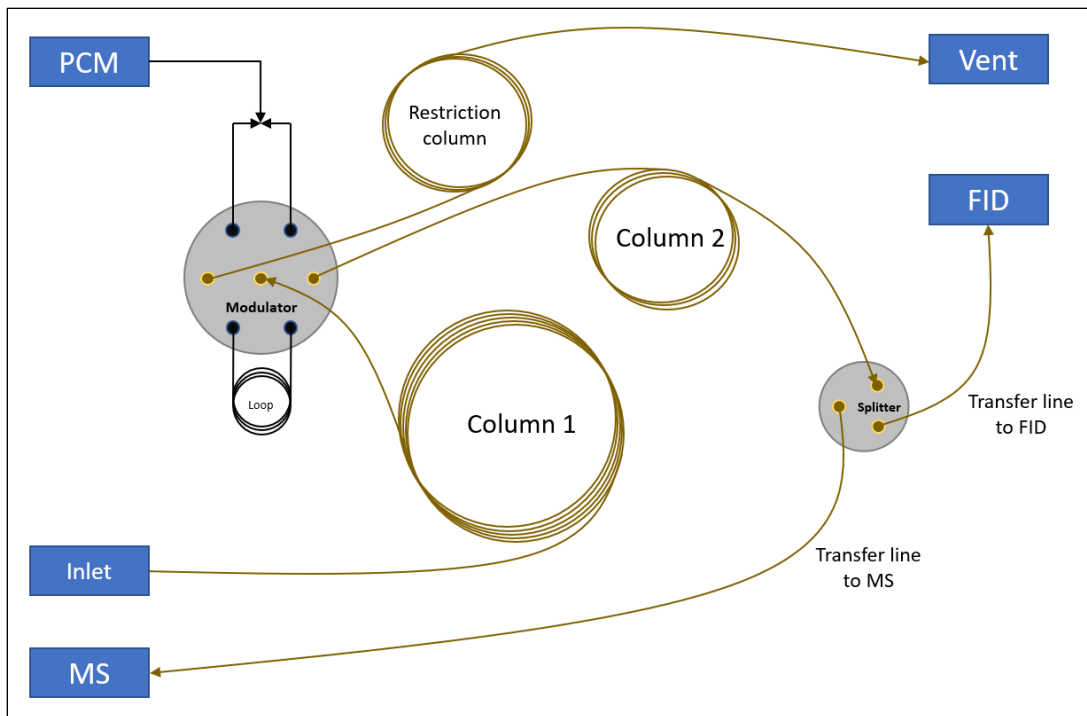


Figure 3: Column configuration in the GCxGC set-up applied during this project. Primary column from inlet to modulator, secondary column from modulator to splitter, transfer lines from splitter to FID & MS, restrictor column connected to modulator for venting and PCM connected to modulator to regulate flow through secondary- and restriction column.

2.2.2 Modulators

The modulator collects fractions of effluent from the primary column in a sample loop and reinjects them into the secondary column. Modulation can be regulated by flow-based modulators or by cryogenic modulators (JSB, n.d.). The modulator that was used during the GCxGC project is a flow modulator. (figure 4). Flow differentials within the modulator facilitate the collection and subsequent reinjection of effluent from the primary column into the secondary column. The speed of the reinjection creates a focusing effect, resulting in very narrow modulated peaks (Agilent Technologies, Inc., 2007).

Flow modulators come in forward flow and reversed flow variants. In a forward flow modulator, the sample loop is filled and flushed in the same direction. In a reversed flow modulator, these directions are opposite to each other, as illustrated in figure 4. The application of a reversed flow modulator results in a much lower baseline compared to when a forward flow modulator is applied. This is the case, because a forward flow modulator is much more prone to leaking of effluent from the primary column into the secondary column (JSB, n.d.).

During the GCxGC project a reversed flow modulator was used. Its function is as follows: during fill mode (figure 4, left), the effluent exiting from the primary column is directed into the sample loop. At the same time, the pneumatic control module (PCM) directs a high flow of helium towards the secondary column. The content of the sample loop is injected into the secondary column during the flush mode. The PCM directs helium towards the restrictor column and secondary column (figure 4, right). (Agilent Technologies, Inc., 2007) (JSB, n.d.). The flow rate directed through the secondary column is usually around 20 mL/min. This high flow rate is necessary to elute each fraction in time before the next fraction is ready to be injected. A typical second dimensional separation takes 3-5 seconds (Ong & Marriott, 2002).

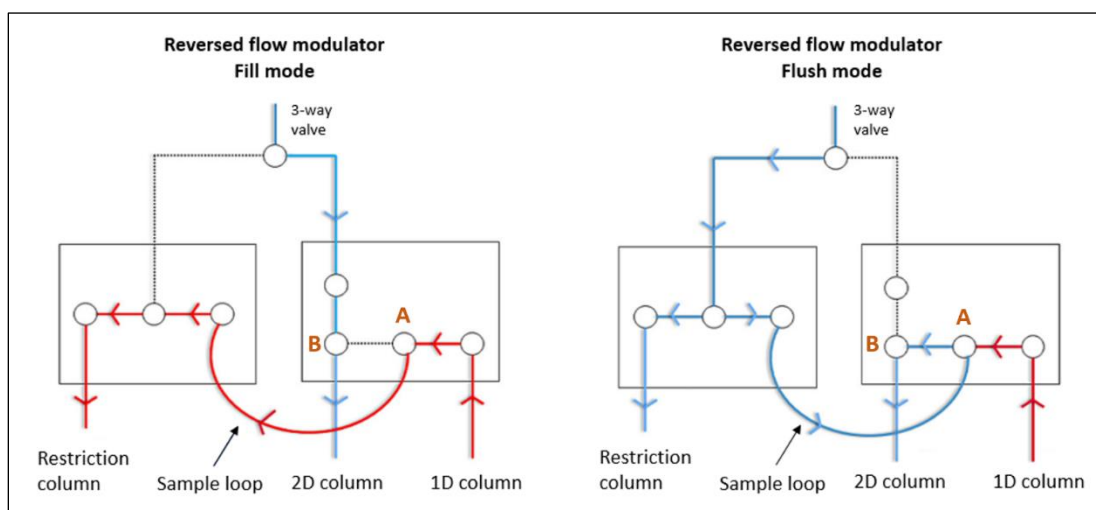


Figure 4: Schematic depiction of the reversed flow modulator and its function. Fill mode: effluent from primary column through loop to restriction column, high helium flow from PCM directly to secondary column. Effluent from primary column is blocked at point B. Flush mode: high helium flow from PCM through loop to secondary column and restriction column. Effluent from primary column is blocked at point A (Duhamel et al., 2015b).

The time needed to fill the sample loop is dependent on the volume of the loop and the 1D flow rate. When the time needed to fill the loop for 100% is exceeded, effluent from the primary column will be lost. Loop fill time is therefore usually set at a time in which 75% of the loop is filled. The time needed to flush the loop is dependent on the volume of the loop and the 2D flow rate. When the loop is not sufficiently flushed, effluent will be lost, which is why the loop flush time is usually set at 150% of the time needed to flush the entire loop (Gestel, W. van., GCxGC training Da Vinci, Feb 16, 2022).

2.2.3 Flow rate compatibility and GCxGC operating window

1D- and 2D flow rate compatibility was studied to make sure that undesirable chromatographic effects could be avoided as much as possible during GCxGC/MS method development. The set of compatible 1D- and 2D flow rates resulting from this study is called the GCxGC operating window. After determining the operating window, parameter settings for 1D flow rate, 2D flow rate and oven temperature ramp could be optimized by Design of Experiments (DoE).

It becomes clear that some 1D- and 2D flow rates are not compatible when considering the flow paths within the modulator, as illustrated in figure 4. During the fill stage, effluent from the primary column flows into the sample loop and helium flows from the PCM directly towards the secondary column (figure

4, left). During the flush stage, helium flows from the PCM through the sample loop towards the secondary column. Effluent from the primary column is temporarily blocked by this high flow of helium at point A (figure 4, right). The effluent flow during both these stages and the quality of the resulting chromatogram, can be negatively affected by at least two types of 1D and 2D flow rate combinations (Gestel, W. van., GCxGC training Da Vinci, Feb 16, 2022).

The first type is a combination in which the 2D flow rate is too low for the 1D flow rate. The 2D flow rate is then not high enough to hold back the effluent from the primary column at point B during fill mode and point A during flush mode (figure 4), causing the effluent from the primary column to leak into the secondary column. This type of flow rate combination can result in tailing and in an effect called 'streaking'. Streaking occurs when an analyte eluting from the primary column is continuously introduced into the secondary column, instead of in fractions, resulting in continuous detection. The effect is called streaking because analytes appear in the chromatogram as vertical lines/streaks. (Gestel, W. van., GCxGC training Da Vinci, Feb 16, 2022).

The second type of 1D and 2D flow rate combination that negatively affects the quality of the chromatogram is when the 1D flow rate is too low for the 2D flow rate. This type of combination results in the 2D flow not only preventing streaking, but also preventing proper elution from the primary column into the sample loop. Eventually, no peaks are invisible anymore in the chromatogram, because a 1D peak is cut up in too many small fractions. (Gestel, W. van., GCxGC training Da Vinci, Feb 16, 2022).

The combinations of 1D- and 2D flow rates that resulted in chromatograms that are not affected by the abovementioned effects were included within the operating window. When applying these flow rate combinations, the 1D effluent can pass point A, but is unable to pass point B during the loop fill stage (figure 4, left). The 1D effluent is unable to pass both point A and B during the loop flush stage (figure 4, right).

2.2.4 GCxGC columns

One column pair was selected for the GCxGC/MS method development project. Both the primary and secondary column were therefore not optimized. This paragraph addresses the specifications of these columns and how they relate to other available options, because the selection and application of the correct column pair is critical to fully exploit the capabilities of GCxGC.

Column selection and installation are dependent on the nature of the sample and on the objectives of the analyst. Aspects such as the polarity of the columns and the order in which they are connected must be considered as well as chemistry of the stationary phase and column dimensions. The combination of a 20-60 m, narrow bore, non-polar 1st dimensional column and a 1-5 m, narrow bore, polar 2nd dimensional column is most commonly used. However, for some applications the opposite order of combination or different column dimensions are desirable to maximize separation and peak capacity (Mostafa et al., 2012).

To achieve the enhanced separation and peak capacity that GCxGC can provide, a combination of two independent retention mechanisms must be applied. When two independent retention mechanisms are combined, the GCxGC system is said to be orthogonal. To create an orthogonal GCxGC system, a non-polar column is installed as the primary column and the polar column is installed as the secondary column. The analytes are then separation based on boiling point in the first dimension and based on polarity in the second dimension. When installing a polar column in the first dimension, separation over the first column will be based on both boiling point and polarity, and based on polarity in the second dimension, as separation in the first dimension occurs during a temperature ramp and separation in the second dimension is practically isothermal. In this case, the column pair is orthogonal, but the GCxGC system is nonorthogonal (Omais et al., 2011).

A greater orthogonality of the GCxGC system is usually desirable, as it provides a better overall separation and usage of separation space (Cordero et al., 2006). In chromatography, the term orthogonality is not only used to describe column pairs and GCxGC systems, but also to describe to what degree this separation space is exploited. An even distribution of the analytes is desirable. To achieve this, not only the orthogonality of the GCxGC system, but also parameters such as flow rate and oven temperature ramp play an important role (Omais et al., 2011).

As said, column selection for the GCxGC system is highly dependent on the nature of the sample. Some target analytes may be sufficiently separated when applying a less orthogonal system (Mostafa et al., 2012), (Restek, 2022). Combinations of polar primary columns and non-polar secondary columns are uncommon, but have for example been used in the analysis of polyaromatic hydrocarbons in crude oil and cannabinoids in marijuana (Restek, 2012). A combination of a non-polar primary column and a polar secondary column is most commonly used. This type of combination was selected for this project because the composition of DAAs in terms of VOCs was largely unknown and there were no specific target analytes selected. The stationary phase of the primary column consisted of 5% phenyl polysilphenylene-siloxane (BPX5) and the stationary phase of the secondary column consisted of 50% phenyl polysilphenylene-siloxane (BPX50). The chemical structure of both stationary phases is illustrated in figure 5.

Separation over a BPX5 column occurs mainly based on boiling point, as 95% of its stationary phase is made up of non-polar polysilphenylene siloxane and only 5% of the more polar poly(methylphenyl siloxane). A BPX50 column is much more polar because its stationary phase consists for 50% of polysilphenylene-siloxane and for 50% of poly(methylphenyl siloxane) (figure 5). Separation is in this case largely based on pi-pi interactions and partially on H-bonding. Boiling points still play a significant role, though (SGE Analytical Science, n.d.). The incorporation of phenyl into the main chains of the stationary phase give these types of columns a major advantage in terms of thermal stability (Libretexts, 2020).

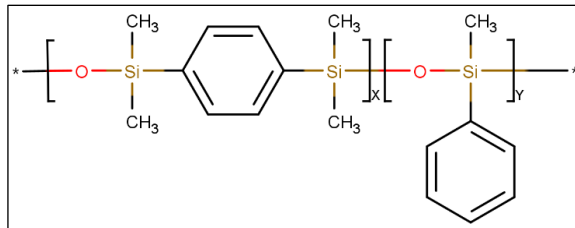


Figure 5: Chemical structure of phenyl polysilphenylene-siloxane stationary phase with repeating units X and Y making up 95% and 5%, respectively, in a BPX5 column and 50% for both units in a BPX50 column (Own work).

There is a wide variety of other stationary phases that can be selected for GCxGC analysis. Of these, 100% dimethyl polysiloxane is commonly used to separate analytes solely based on boiling point. In more polar columns, stationary phases can for example consist of cyanopropylphenyl siloxane, cyanopropyl polysilphenylene siloxane and polyethylene glycol. (SGE Analytical Science, n.d.). Besides orthogonality and chemistry of stationary phases, the dimensions of a GCxGC column pair play an important role. Parameters to consider are column length, inner diameter (I.D.) and film thickness (D_f). These dimensions usually differ significantly between the primary and secondary column because both require different types of performances.

Which dimensions are selected for the column pair is dependent on the nature of the sample and on the objective of the analyst. For first dimensional separation, columns of between 20 and 60 meters are commonly used (Mostafa et al., 2012). For some samples, a long column may be necessary and for some a short column will suffice. For this project, a 20 m, 180 μ I.D., 0.18 μ D_f primary column was selected, based on advice of the supplier. This column has a higher efficiency than a more commonly used 30m, 250 μ I.D., 0.25 μ D_f column (Shimadzu, 2012). The increase in efficiency results from increased interaction frequency between analyte and stationary phase due to the narrower bore and accelerated mass transfer due to the thinner film (Woodward, 2020). A downside of a shorter, narrower bore column is its lower sample loading capacity (Dömötörövá et al., 2006).

The secondary column is required to perform at least three separations per peak eluting from the primary column (Mostafa et al., 2012), (Shimadzu, 2012). Fast separation is therefore needed, which is realized not only by applying a high flow rate, but also by using a relatively short (1-5 m), narrow bore (100-180 μ m) column. For the GCxGC project, a 5 m, 250 μ m I.D., 0.25 μ m D_f secondary column was used. While the application of a column with a narrower bore produces fast and efficient separations in principle, it also makes the second dimension much more prone to overloading (Harynuk et al., 2005). Studies have shown that the performance of narrower bore columns in the second dimension is often similar to that of wider bore columns, and sometimes even better (Shimadzu, 2012).

2.3 Thermal desorption

The thermal desorption (TD) of VOCs by the thermal desorption unit (TDU) is a process that always took place in combination with pyrolysis during this project, and is therefore briefly discussed. The TDU is mounted on the cooled injection system (CIS) inlet of the GC. A cross section of the TDU used during this project combined with a CIS is illustrated in figure 6. VOCs can be desorbed from a sample in the TDU. The CIS focusses the desorbed VOCs in a small band prior to injection (GERSTEL Inc., 2018). During pyrolysis, the position of the sample tube (figure 6) is occupied by the pyrolysis module (figure 7), as explained in further detail in the next paragraph.

3rd party image
and therefore blanked

Figure 6: Cross section of thermal desorption unit (TDU) and cooled injection system (CIS) (SRA Instruments, 2021).

2.4 Pyrolysis

Pyrolysis is the thermal decomposition of materials by application of heat and is especially useful for the study of nonvolatile macro molecules, such as polymers. It is carried out in a pyrolysis module located in the TDU (figure 6). Samples can be inserted into the pyrolyzer with a transport adapter to which a quartz sample holder is secured, as illustrated in figure 7. The pyrolysis coil in the module can heat samples up to temperatures between 350°C and 800°C. Applying heat in this temperature range causes molecules to split at their weakest points, creating smaller, more volatile fragments called pyrolysates. These fragments are called ‘marker pyrolysates’ when they are unique for a certain material and can contribute to the distinction between different materials. The pyrolysates are separated by means of gas chromatography (GC) and detected by means of for example MS or FID. Depending on the sample composition, a wide variety of pyrolysates can be formed during pyrolysis, which results in complex chromatograms. (Mettler-Toledo International Inc., 2020). The sample preparation necessary for pyrolysis was minimal and consisted of milling the EMC to a fine powder to ensure homogenic sampling and fast heat distribution (GERSTEL GmbH & Co.KG, 2022).

3rd party image
and therefore blanked

Figure 7: Quartz sample holders, transport adapters and pyrolysis module used during pyrolysis (Gerstel GmbH & Co. KG, 2011).

Pyrolysis can be carried out in pulsed- and in smart ramp mode. Both these modes have been investigated during the pyrolysis project. During pulsed pyrolysis, the sample is heated to one or more temperatures (initial temperature(s)) with a heating rate of 500°C/s and is usually held there for several seconds (initial time). Both an initial temperature and an initial time have been selected for pulsed pyrolysis of EMCs. A schematic illustration of the temperature profiles of TD in combination with pulsed pyrolysis is provided in figure 8. (GERSTEL GmbH & Co.KG, 2022).

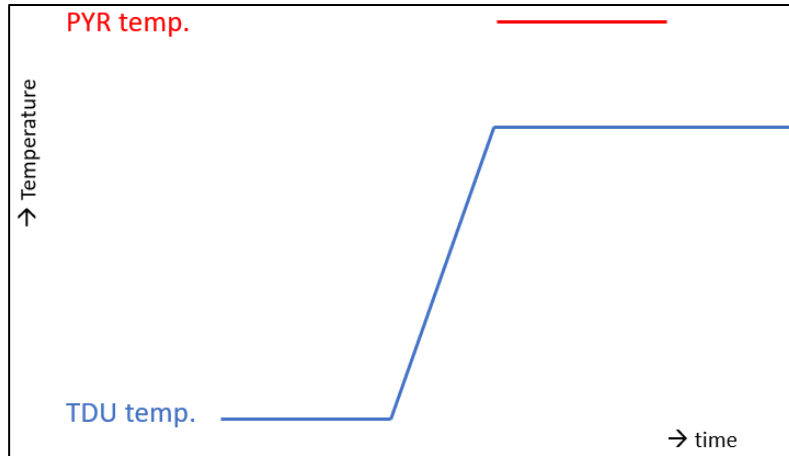


Figure 8: Illustration of thermal desorption and pyrolysis temperature profiles during the application of pulsed pyrolysis (Own work).

During smart ramp pyrolysis, an end temperature is reached with a low heating rate of 5°C/s following the TD ramp and is held there for usually several seconds (initial time) (GERSTEL GmbH & Co.KG, 2022). Both an end temperature and initial time have been selected for smart ramp pyrolysis of EMCs, using the same approach as for pulsed pyrolysis. A schematic illustration of the temperature profiles of TD in combination with smart ramp pyrolysis is provided in figure 9.

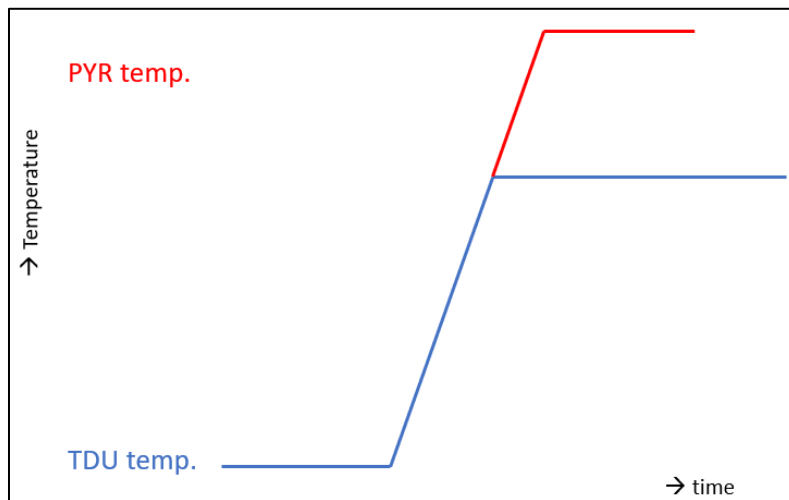


Figure 9: Illustration of thermal desorption and pyrolysis temperature profiles during the application of smart ramp pyrolysis (Own work).

2.5 Thermogravimetric analysis by evolved gas analysis

Thermogravimetric analysis (TGA) can provide valuable information about the decomposition temperatures of materials. This kind of data is useful in PYR-GC/MS method development. It is important to reach the decomposition temperature of the components in the sample, but also not exceed it by much. Exceeding the decomposition temperature can lead to loss of chemical information and to secondary reactions between pyrolysates. Optimal pyrolysis temperatures can be derived from TGA data (Kleine Benne, E. & Zhou, H. X., Gerstel GmbH & Co. KG, video lecture on pyrolysis).



Research by Stuff et al. (2012) has pointed out that TGA can be reliably simulated by PYR-GC/MS. This type of operation is also referred to as evolved gas analysis (EGA). First, a sample undergoes thermal treatment to outgas and pyrolyze its constituents, after which the gaseous components are transferred towards the FID detector through a non-retaining, deactivated fused silica column. The amount of gas eluting from the column can be correlated to the temperatures applied in the TDU and pyrolysis module (Stuff et al., 2012). Research has shown that EGA data can be reliably used to determine optimal pyrolysis temperatures (Ma et al., 2014). The initial temperatures for pulsed pyrolysis and end temperature for smart ramp pyrolysis were therefore determined by applying EGA.

3. Experimental

The chemicals and materials used during both the GCxGC and pyrolysis project are listed in paragraph 3.1, followed by instruments, equipment and software in paragraph 3.2. Paragraphs 3.3 and 3.4 cover the experimental set-up for the GCxGC/MS and PYR-GC/MS method development, respectively.

3.1 Chemicals and materials

The chemicals and materials used during both projects are listed in table 2.

Table 2: An overview of the chemicals and materials with brand and type/purity that will be used during this project.

Chemical/material	Brand	Type/purity/concentration
Liquid nitrogen	Cryosolutions	N.A.
Helium gas	Air Liquide	4N
Epoxy molding compounds ¹	A, B and C	1 (MAR), 2 (MAR) and 3 (ECN)
Die attach adhesives ¹	X	1
Acetone	Merck	99.8 %
Standard mixture: toluene, octane, p-xylene, decane, 2-pyrrolidinone 1-methyl, triethyl phosphate, hexadecane, tri(2-chloroethyl) phosphate, phthalic acid	N.A.	500 ng/μL for each compound

1. The brands and types of samples are indicated with letters and numbers, respectively, due to confidentiality.

3.2 Instruments, equipment and software

The instruments, equipment and software used during both projects are listed in table 3.

Table 3: An overview of instruments, equipment and software with brand and type that will be used during this project.

Instrument/equipment/software	Brand	Type
Gas chromatograph with S/SL inlet and PTV inlet (new system)	Agilent Technologies	8890B
Gas chromatograph with S/SL inlet and PTV inlet (old system)	Agilent Technologies	6890A
Analytical capillary GC column	Agilent Technologies	J&W VF-1ms, 30 m, 0.25 mm I.D., 1.00 μm D _f 100% dimethylpolysiloxane
¹ D Analytical capillary GC column	SGE Analytical Science	BPX5, 20 m, 0.18 mm I.D., 0.18 μm D _f , 5% phenyl polysilphenylene-siloxane
² D Analytical capillary GC column	SGE Analytical Science	BPX50, 5 m, 0.25 mm I.D., 0.25 μm D _f , 50% phenyl polysilphenylene-siloxane
Deactivated fused silica capillary tubing	Agilent Technologies	Deactivated Fused Silica, High Temp, 5 m, 0.25 mm I.D.
Flame Ionic detector (FID)	Agilent Technologies	Optimized for capillary
Mass Selective Detector (MS) with Ei extractor-ion source (new system)	Agilent Technologies	5977B
Mass Selective Detector (MS) (old system)	Agilent Technologies	5973N
GCxGC Flow modulator	Sepsolve	Reversed flow modulator
Cooled Injection System (CIS)	GERSTEL	CIS4
Thermal Desorption Unit (TDU)	GERSTEL	TDU2
Pyrolysis module	GERSTEL	N.A.
Multipurpose Sampler (MPS)	GERSTEL	MPS Robotic XL
GCxGC data processing software	Chromspace	N.A.
Statistical software	Minitab®	Version 20.1.3.0

3.3 GCxGC/MS method development and application

The method development for qualitative GCxGC/MS analysis of VOCs in DAAs was carried in five phases, as listed below. The experimental set-up of these phases is discussed in more detail in the paragraphs following.

- 1. Determination of GCxGC operating window.** The compatibility of 1D and 2D flow rates was investigated.
- 2. Determination of DoE factor ranges.** Factor ranges for 1D flow rate, 2D flow rate and oven temperature ramp were defined. Aspects such as analysis time, peak area, peak height, and 1D/2D flow rate compatibility were considered.
- 3. Execution of DoE and selection of optimal settings.** 1D flow rate, 2D flow rate and oven temperature ramp were optimized by means of Experimental Design. 1D Resolution, 2D resolution and peak area served as responses.
- 4. Assessment of repeatability.** The repeatability of peak area for GCxGC/MS analysis was determined.
- 5. Single column GC versus GCxGC.** The results of single column GC/MS- and GCxGC/MS analysis of DAA 1 were compared with regard to compound separation and compound identification.

3.3.1 Determination of GCxGC operating window

The GCxGC operating window was determined by considering 1D/2D flow rate compatibility, as discussed in paragraph 2.2.3. To determine the operating window, 1D flow rates from 0.4 to 0.65 mL/min were combined with 2D flow rates of 15 to 27.5 mL/min. All analyses were carried out with an oven temperature ramp of 6°C/min. Some of the analyses were also carried out with a 3°C/min oven temperature ramp. Loop fill times and loop flush times were set at 75% and 150%, respectively, and were calculated according to the applied 1D- and 2D flow rates (Gestel, W. van., GCxGC training Da Vinci, Feb 16, 2022). An overview of all the 1D- and 2D flow rate combinations, modulation times and oven temperature ramps applied during this phase is provided in appendix 3. Example calculations for both loop fill time and loop flush time are provided in appendix 4. The parameter settings for GCxGC/MS and liquid injection that remained unchanged during this phase are listed in white in appendix 2.

A 500ng/μL standard mixture (table 1) was used to define the operating window to account for a variety of boiling points and polarities. Using liquid injection for GCxGC/MS method development made it possible to carry out numerous analyses after preparing only one solution. The effects of parameters settings could also be studied more reliably by constantly introducing the same solution. Flow rate combinations that resulted in chromatograms without any undesirable chromatographic effects were included in the operating window. Streaking and a total absence of peaks were expected to be encountered, as discussed in paragraph 2.2.3 (Gestel, W. van., GCxGC training Da Vinci, Feb 16, 2022). After the determination of the operating window, the factor ranges for the DoE were determined.

3.3.2 Determination of DoE factor ranges

Within the operating window, parameter settings for 1D flow rate, 2D flow rate and oven temperature were optimized by means of Experimental Design. The range for the factors was determined in the following way.

Oven temperature ramp

The lower limit of the oven temperature ramp was set at 3°C/min. This resulted in an analysis of approximately 1.5 hours, which is the maximum amount of time NXP wished to spend. The upper limit of the oven temperature ramp was set at 6°C/min. A higher temperature ramp would likely compromise the quality of the chromatogram, as discussed in paragraph 2.2.1.

1D- and 2D flow rates

The determination of the upper and lower limits of 1D- and 2D flow rates was carried out in two phases. First, the peak height and peak area of p-xylene in the standard mixture (table 1) was determined with the set of compatible 1D- and 2D flow rate combinations listed in table 4. The flow rate combinations were selected based on the operating window that was previously determined. The peak height and peak area of p-xylene were recorded and the data was used to indicate which flow rate combination would result in the detection of the largest amount of analyte. The analyses listed in table 4 were carried out with an oven ramp of 3°C, a 75% loop fill time and 150% loop flush time. The remaining parameter settings for GCxGC/MS and liquid injection applied during this phase are listed in white in appendix 2.

Table 4: An overview of the analyses carried out to determine the factor ranges for 1D- and 2D factor ranges. The analyses were carried out with an oven ramp of 3°C, a 75% loop fill time and 150% loop flush time.

Analysis	1D flow rate (mL/min)	2D flow rate (mL/min)
1	0.4	15
2	0.45	17.5
3	0.5	20
4	0.55	22.5
5	0.6	25
6	0.65	27.5

Based on the results of the first phase, a center point for the flow rate factor ranges was selected. The upper and lower limit for 1D- and 2D flow rate followed from 1D- and 2D flow rate compatibility. The factor ranges were extended until the flow rates were likely to be not compatible anymore.

3.3.3 Execution of DoE and selection of optimal settings

A trial analysis of DAA 1 resulted in a separation of components in both the first and second dimension. For this trial analysis, 1D-, 2D flow rate and oven temperature ramp were 0.5 mL/min, 20 mL/min and 3°C/min, respectively. Loop fill times and loop flush times were set at 75% and 150%, respectively, and were calculated according to the applied 1D- and 2D flow rates. The remaining parameter settings for GCxGC/MS analysis are listed in white in appendix 2. The sample solution for DAA 1 was prepared by dissolving about 200 mg DAA in about 20 mL acetone. The sample mixture was centrifuged and subsequently filtered over a 0.45µm filter.

Because of the observed separation in both dimensions after the trial analysis, DAA 1 was used to determine the optimal settings for 1D flow rate, 2D flow rate and oven temperature ramp by means of Experimental Design. 1D resolution and 2D resolution and peak area served as responses. The factors and their corresponding level values are listed in table 5. The settings for the factors in table 5, as well as the applied modulation times, are listed in appendix 7.

Table 5: Three level DoE with factors 1D flow rate (mL/min), 2D flow rate (mL/min) and oven temperature ramp (°C/min).

Factor	Level 1	Level 2	Level 3
1D flow rate (mL/min)	0.475	0.5	0.525
2D flow rate (mL/min)	19	20	21
Oven temperature ramp (°C/min)	3	4.5	6

Each analysis in the DoE was carried out with 75% loop fill time for the highest 1D flow rate in the set, to prevent loss of analyte. The time needed to flush the loop 150% when operating at the lowest 2D flow rate was set as the loop flush time for the entire set, to prevent insufficient flushing. This was necessary because modulation times were set in separate tool without the opportunity to create a sequence. The effects of parameter settings, as well as factor interactions and suggestions for optimal settings were studied using Minitab®. The optimal settings for the general GCxGC/MS method were selected based on these data analyses and a final examination of streaking effects.

3.3.4 Assessment of repeatability

The developed GCxGC/MS method was applied to determine the repeatability of peak area. DAA 1 was analyzed in tenfold by GCxGC/MS and in fivefold by GCxGC/FID. The parameter settings of the developed GCxGC/MS method are listed in appendix 2.

3.3.5 Single column GC versus GCxGC

DAA 1 was analyzed with the single column GC/MS method currently used at NXP and with the newly developed GCxGC/MS method. This was done to determine if there was any additional value of GCxGC analysis compared to single column GC with regard to compound separation and compound identification. Single column GC/MS analysis was carried out on the old GC/MS system and GCxGC/MS analysis was carried out on the new GC/MS system (table 3). The parameter settings for single column GC/MS are listed in appendix 1. The parameter settings of the developed GCxGC/MS method are listed in appendix 2. The DAA samples were prepared as discussed in paragraph 3.3.3.

3.4 Pyrolysis-GC/MS method development and application

Method development for PYR-GC/MS was carried out in two stages. First, evolved gas analysis (EGA) was carried out to determine the main decomposition temperatures of the materials in EMC 1-3. The EGA data was used to select initial temperatures for pulsed pyrolysis and an end temperature for smart ramp pyrolysis. The influence of the pyrolysis duration on the results of pulsed PYR-GC/MS was investigated during the second phase and an initial time was subsequently selected. All three EMCs were analyzed with the developed PYR-GC/MS method in pulsed mode to determine the applicability of the resulting chromatograms as fingerprints and to explore the possibilities for material characterization. Smart ramp pyrolysis was carried out only once to enable a comparison with the results of pulsed pyrolysis.

3.4.1 Pyrolysis temperatures from evolved gas analysis

Thermogravimetric analysis (TGA) was simulated by carrying out evolved gas analysis to find pyrolysis temperatures for both pulsed- smart ramp pyrolysis. Three EMCs underwent thermal treatment to outgas and pyrolyze their constituents. The gaseous components were transferred through a non-retaining deactivated fused silica column towards the FID detector. FID sufficed for EGA and was used instead of MS to protect the MS against fouling. The determination of pyrolysis temperatures by EGA was based on research carried out by Stuff et al. (2012) commissioned by GERSTEL, and on the information gained during the training given by Da Vinci at NXP on the principles of pyrolysis (Gestel W. van., Da Vinci Laboratory Solutions, pyrolysis training, Feb 17, 2022). Sample preparation and analysis conditions are listed below, followed by a graphical representation of the EGA temperature program.

Sample preparation

Approximately 5 mg of each EMC was milled to a fine powder using a ball miller and transferred into a quartz, test-tube shaped pyrolysis vessel (figure 7).

Analysis conditions

TDU	70 °C (hold 1.0 min); 0.17 °C/s to 350°C (hold 47 min)
Pyrolysis	80 °C (1 min); 0.17 °C/s to 800 °C (hold 2 min)
CIS	250°C (hot split) Split 1:50
Column	5 m Deactivated Fused Silica tubing, D.I. = 0.250 mm
Pneumatics	He, constant flow = 1.2 mL/min
Oven	40°C to 250°C (7°C/min), hold 50 min
FID	Frequency: 200Hz

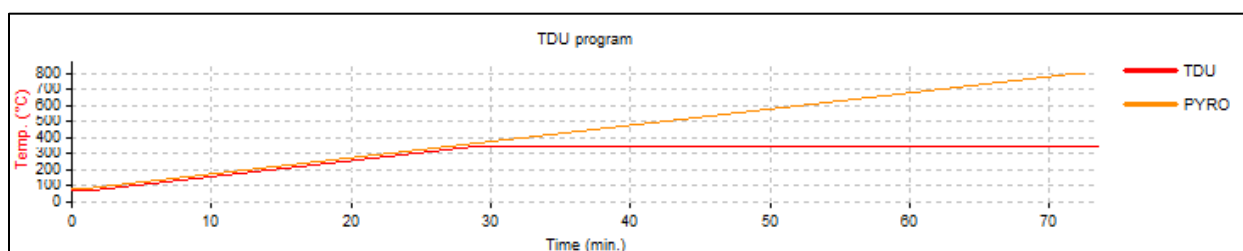


Figure 10: Graphical representation of EGA temperature program. TD initial temperature: 70°C, TD initial time: 1 min, TD temperature rate: 0.17°C/sec, TD end temperature: 350°C, 47 min hold. PYR initial temperature: 80°C, PYR temperature rate: 0.17°C/s, PYR end temperature: 800°C, 2 min hold.

3.4.2 Selection of pyrolysis duration and application of PYR-GC/MS

PYR-GC/MS analyses of EMC were carried out in pulsed mode (figure 8) and in smart ramp mode (figure 9). The parameter settings applied during PYR-GC/MS are listed in appendix 21, in which the final settings of the investigated parameters are highlighted in green. The conditions for pyrolysis itself are discussed in more detail below. Samples were prepared as discussed in paragraph 3.4.1.

Pulsed pyrolysis

The initial temperatures 425°C and 575°C were selected for pulsed pyrolysis based on the EGA data. These temperatures were applied consecutively during each pulsed pyrolysis run. Initial times of 12, 18 and 24 seconds were applied to EMC 1 to investigate the influence of pyrolysis duration. Pulsed pyrolysis of EMC 1 with an initial time of 12 seconds was carried out in triplo to determine repeatability. EMC 2 and 3 were analyzed only once, and with an initial time of 12 seconds. A graphical representation of the temperature program for pulsed pyrolysis is illustrated in figure 11.

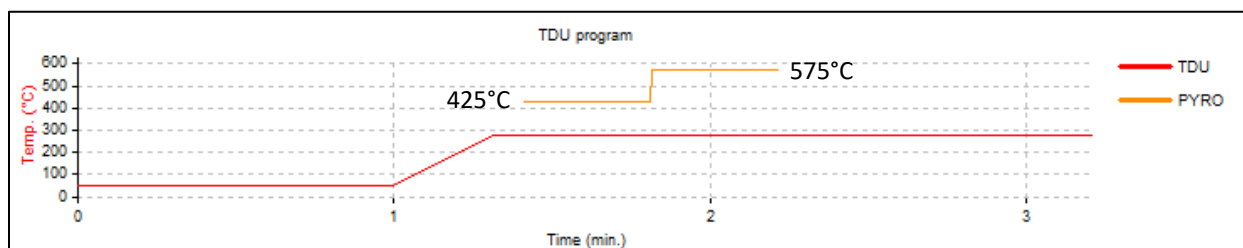


Figure 11: Graphical representation of temperature program for pulsed pyrolysis of EMCs. TD initial temperature: 40°C, TD initial time: 1 min, TD temperature rate: 12°C/sec, TD end temperature: 280°C, PYR initial temperature 1: 425°C, PYR temperature rate: 500°C/s, PYR initial temperature 2: 575°C. Initial times of 12, 18 and 24 seconds were applied.

Smart ramp pyrolysis

Smart ramp PYR-GC/MS was carried out once for EMC 1 to compare the resulting chromatogram with the chromatograms resulting from pulsed PYR-GC/MS. The end temperature selected was 625°C and initial time was 12 seconds. A graphical representation of the temperature program for smart ramp pyrolysis is illustrated in figure 12.

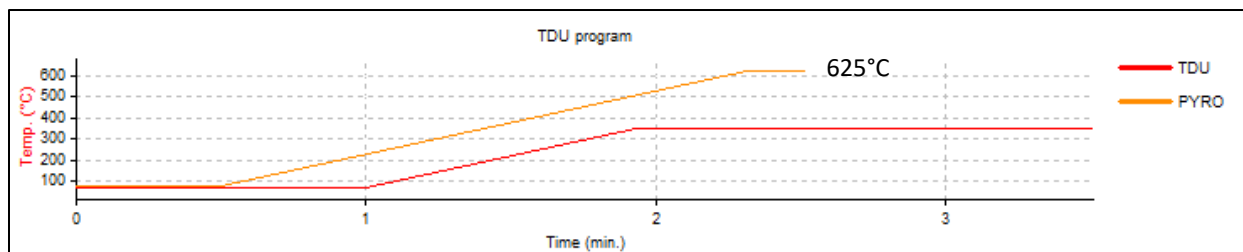


Figure 12: Graphical representation of temperature program for smart ramp pyrolysis of EMCs. TD initial temperature: 70°C, TD initial time: 1 min, TD temperature rate: 5°C/sec, TD end temperature: 350°C, PYR initial temperature: 80°C, PYR temperature rate: 5°C/s, PYR end temperature: 625°C, PYR initial time: 12 seconds.

4. Results

The results of two separate method development projects are presented in this chapter. The results of GCxGC/MS method development will be addressed first, followed by the results of PYR-GC/MS method development.

4.1 GCxGC/MS method development and application

The presentation of the results for GCxGC/MS method development is structured similarly to the experimental section of this project. The determination of the operating window was essential for optimization of 1D- and 2D flow rates and will be addressed first. Optimization of 1D flow rate, 2D flow rate and oven temperature ramp is then discussed by first addressing the determination of DoE factor ranges. The analysis of the DoE data and resulting optimal parameter settings are discussed in the paragraph following. The final two paragraphs cover repeatability of GCxGC/MS results, and the comparison between single column GC/MS and GCxGC/MS with regard to compound separation and reliability of compound identification.

4.1.1 GCxGC operating window

The GCxGC operating window is defined during this project as the set of compatible 1D- and 2D flow rates. The scope of the operating window was limited by the occurrence of four undesirable effects. These include streaking, absence of peaks, lack of retention in the second dimension and MS fouling. The occurrence of streaking and absence of peaks were expected prior to the experimental phase. The causes of these effects are discussed in paragraph 2.2.3. Lack of retention in the second dimension and MS fouling were encountered during the experimental phase. The four effects limiting the scope of the operating window are discussed in more detail below. The final operating window is illustrated in figure 15.

1. Streaking

Streaking effects are encountered when a too high 1D flow rate is combined with a too low 2D flow rate. Effluent from the primary column leaks into the secondary column when such a combination is used, resulting in continuous detection. Figures 13 and 14 illustrate partial GCxGC chromatograms generated during the determination of the operating window.

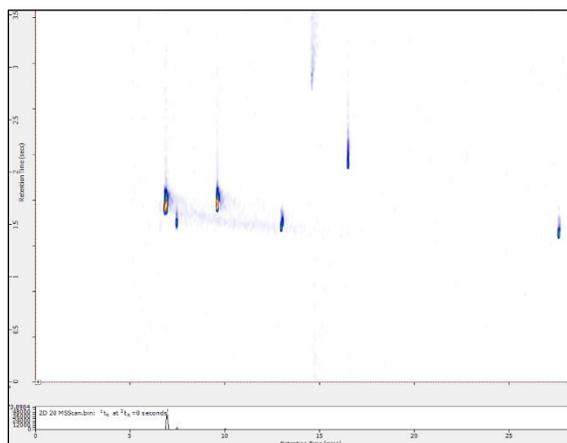


Figure 13: GCxGC chromatogram of standard mixture where no streaking occurs. 1D flow rate is 0.5 mL/min and 2D flow rate is 20 mL/min (own work).

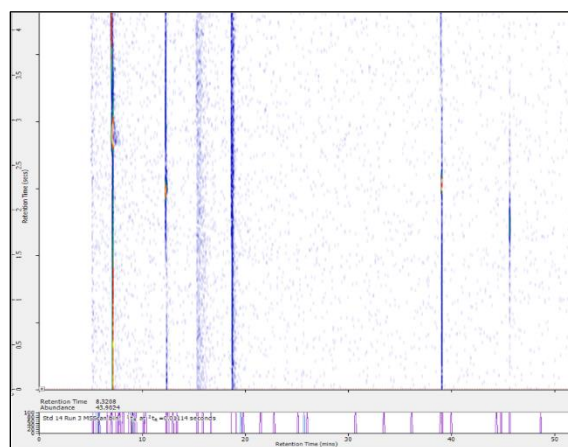


Figure 14: GCxGC chromatogram of standard mixture where streaking does occur. 1D flow rate is 0.6 mL/min and 2D flow rate is 15 mL/min (own work).

Figure 13 illustrates a chromatogram free of streaking. A 0.5 mL/min 1D flow rate and a 20 mL/min 2D flow rate were applied here. The 1D- and 2D flow rates are compatible and the combination is highlighted in green in the diagram in figure 15. Figure 14 illustrates a chromatogram where streaking is observed. In this case, a 1D flow rate of 0.6 mL/min was combined with a 2D flow rate of 15 mL/min. This flow rate combination results in streaking effects and is therefore highlighted in red in the diagram in figure 15.

2. Absence of peaks

Chromatograms may display no peaks at all when combining a 1D flow rate that is too low with a 2D flow rate that is too high. The set of 1D- and 2D flow rate combinations where this effect occurred is highlighted in gray in figure 15.

3. No 2D retention

The cells highlighted in orange in figure 15 indicate flow rate combinations that resulted in the detection of analytes without streaking effects, but no retention was observed in the second dimension. This effect is undesirable, as it eliminates the possibility to separate components in the second dimension. Flow rate combinations that resulted in chromatograms showing this effect were therefore excluded from the operating window.

4. Fouling of the MS

Finally, fouling of the MS occurred after applying high flow rate combinations, even if these flow rates were compatible and resulted in acceptable chromatograms. These combinations are highlighted in blue in figure 15. The values in the tuning report that indicated fouling returned to acceptable levels after keeping the instrument idle for 24 hours. It is possible that the amount of analyte introduced into the MS was too high and the vacuum pump was not able to evacuate the excess gas (Sudol et al., 2020).

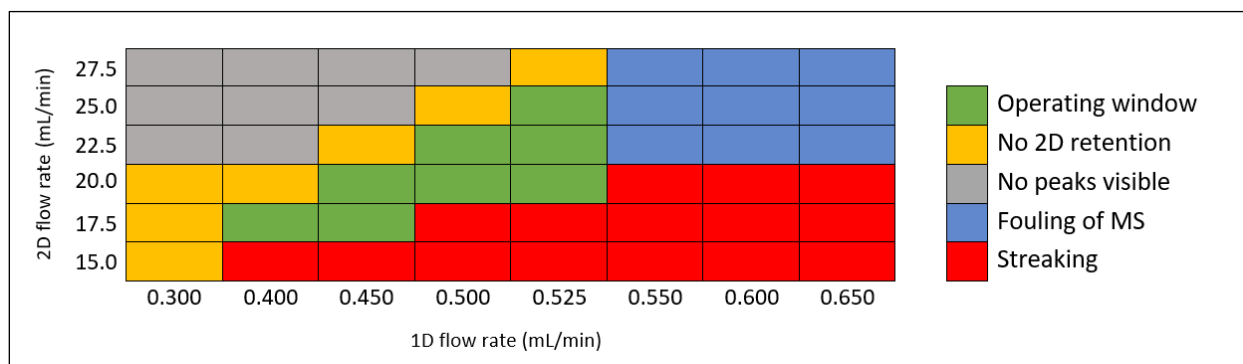


Figure 15: Graphical illustration of the operating window for GCxGC and the undesirable effects encountered around it (own work).

The influence of the oven temperature ramp on the scope of the operating window was investigated as discussed in paragraph 3.3.1 and as indicated in appendix 3. Only one difference was observed between chromatograms acquired with 3°C/min and 6°C/min ramps. Lack of 2D retention was slightly less severe when operating with a 3°C/min ramp. This is expected, because the elution temperature of analytes is lower with this ramp than with a ramp of 6°C/min. This effect is illustrated in the plot in appendix 10.

4.1.2 DoE factor ranges

After the determination of the operating window, the parameter settings for 1D flow rate, 2D flow rate and oven temperature ramp could be optimized. This was realized by mean of Experimental Design. The DoE factor range for the oven temperature ramp was set at 3°C – 6°C, as discussed in paragraph 3.3.2. Factor ranges for 1D- and 2D flow rates were determined after examining the peak area and peak height for p-xylene resulting from a set of compatible flow rates. The results in appendix 5 indicate that there is a relation between the type of flow rate combination and the area and counts measured. The relations are further illustrated in figure 16. Peak height (counts) and peak area (counts•min) of p-xylene are plotted against 1D/2D flow rate combinations (mL/min). The peak height and peak area increase from 0.4/17.5 to 0.5/20, but decrease again from combination 0.5/20 to 0.65/27.5.

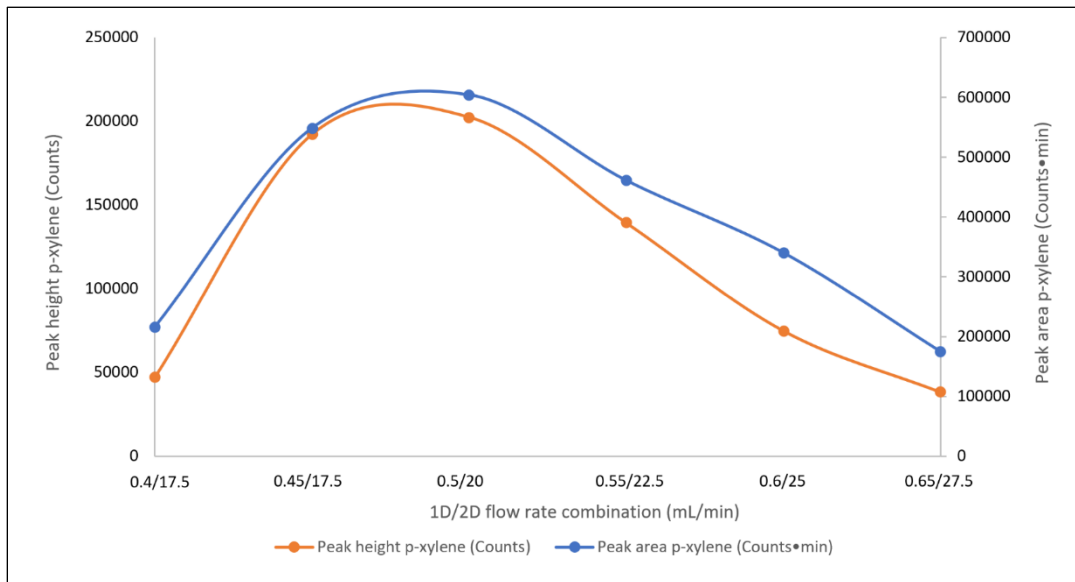


Figure 16: A plot of the counts for p-xylene vs 1D/2D flow rate combination (mL/min) and area of p-xylene (counts•min) vs 1D/2D flow rate combination (mL/min). The data plotted is listed in appendix appendix 5 (own work).

Based on this data, 0.5 mL/min was selected as the center for the 1D flow rate factor range and 20 mL/min was selected as the center for the 2D flow rate factor range. The extent of the factor ranges was based on the scope of the operating window. According to the operating window illustrated in figure 15, a 1D flow rate factor range of 0.45-0.525 mL/min is compatible with a 2D flow rate of 20 mL/min. The 1D flow rate factor range was narrowed to enable the expansion of the 2D flow rate factor range and lower the chance of applying non-compatible flow rates. The 1D flow rate factor range was narrowed to 0.475-0.525 mL/min and the 2D flow rate factor range was set at 19-21 mL/min. The possibility of streaking or other undesirable effects could not be excluded, because the application of 2D flow rates such as 19 and 21 mL/min had not been investigated yet. The ranges for all three factors are summarized in table 6.

Table 6: Three level DoE with factors 1D flow rate (mL/min), 2D flow rate (mL/min) and oven temperature ramp (°C/min).

Factor	Low level	High level
1D flow rate (mL/min)	0.475	0.525
2D flow rate (mL/min)	19	21
Oven temperature ramp (°C/min)	3	6

4.1.3 DoE and selection of optimal settings

A GCxGC/MS analysis of DAA 1 as described in paragraph 3.3.3 resulted in the chromatogram illustrated in appendix 6. A cut-out of this chromatogram is illustrated in figure 17. Retention in the primary column (min) is in the horizontal direction and retention in the secondary column (sec) is in the vertical direction. The cut-out illustrates the additional capabilities that GCxGC has over single column GC in terms of compound separation. In the first dimension, where separation is primarily based on boiling point, component B and C are barely separated and component A appears to coelute with component C. The separation of B, C and D could not be improved over the secondary column, where separation is based on polarity, but component A is now separated from component C. Component A and C may have a similar boiling point, but their polarity is different. The shorter retention time of component A compared to B, C and D indicates that A is less polar than B, C and D.

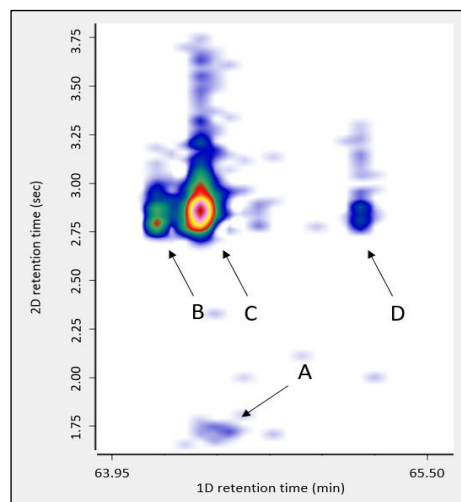


Figure 17: Cut-out of the GCxGC chromatogram of DAA 1, illustrated in appendix 6. Component A, C and D were used to optimize flow rates and oven temperature ramp (own work).

The DoE was carried out at the levels listed in table 5. An overview of the analyses and their parameter settings is provided in appendix 7. The 2D resolution between compounds A and C and 1D resolution between compounds C and D, as well as the peak area of compound C (figure 17) were used as responses in the DoE. The values found for these responses are listed in appendices 7 and 8. An example for the calculation of resolution is provided in appendix 9. The data resulting from the DoE is discussed in more detail below, followed by the selection of optimal parameter settings.

1. 2D resolution AC

The main effects plot for 2D resolution AC illustrated in figure 18 shows that the average response increases as the 1D flow rate increases, decreases as the 2D flow rate increases, and decreases as the oven temperature ramp increases.

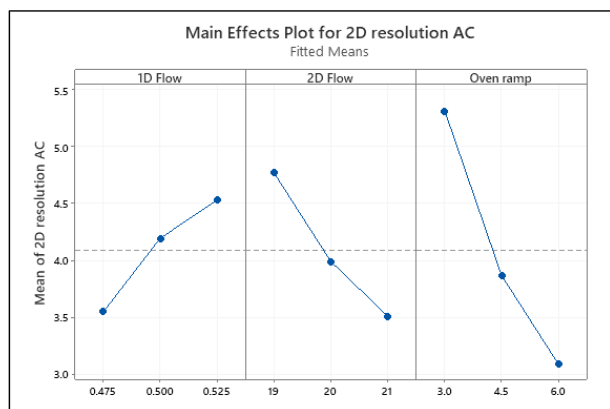


Figure 18: Main effects plot for 2D resolution between A and C. Mean of resolution vs 1D flow rate, 2D flow rate and oven temperature ramp, from left to right (own work).

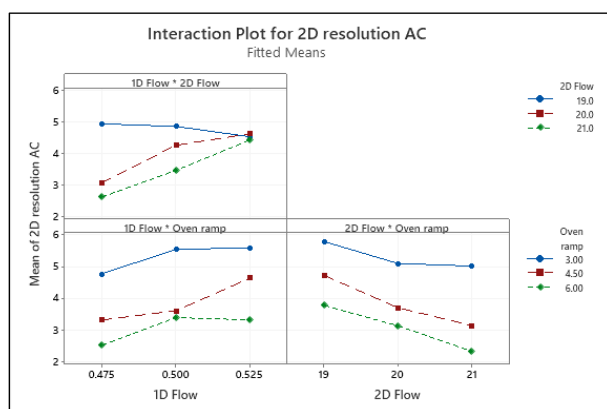


Figure 19: Interaction plot for 2D resolution between A and C. 1D- vs 2D flow rate on top left, 1D flow rate vs oven temperature ramp in bottom left, and 2D flow rate vs oven temperature ramp on the right (own work).

It is important to emphasize that these plots display average resolutions. In fact, the highest resolution was achieved by applying a 1D flow rate of 0.475 mL/min (appendix 8), but the average resolution achieved by applying this 1D flow rate is lower than the average resolution achieved when applying 1D flow rates of 0.500 and 0.525 mL/min. This can be explained by the interaction between the 1D- and 2D flow rate, as illustrated in figure 19.

The interaction between 1D- and 2D flow rate is a great illustration of the significance of 1D/2D flow rate compatibility, as discussed in 2.2.3. The 2D resolution suffers when the lowest 2D flow rate of 19 mL/min is combined with an increasingly higher 1D flow rate. This is probably because the likelihood of streaking becomes greater, resulting in more tailing in the second dimension. On the other hand, combining the higher 2D flow rates with an increasingly higher 1D flow rate results in higher resolution. The interaction between the oven temperature ramp and flow rates is less obvious than between the two flow rates themselves, as indicated in figure 19.

The fact that oven temperature ramp has an influence on the resolution in the second dimension seems counterintuitive. The modulation of a 1st dimensional peak takes only several tens of seconds, and is therefore practically isothermal. But as the oven temperature ramp increases, the modulation of a 1st dimensional peak becomes increasingly non-isothermal. This may result in different retention times in the second dimension within one peak, compromising the 2D resolution. Another explanation for the effect of the oven temperature ramp on the 2D resolution has to do with the elution temperature from the primary column. The elution temperature of a given analyte is higher when a higher temperature ramp is applied, as illustrated in the plot in appendix 10. This causes the separation in the second dimension to take place at a higher temperature as well, which compromises the 2D resolution.

2. 1D resolution CD

The main effects for the 1D resolution between C and D are plotted in figure 20. A slight trend can be observed in which the 1D resolution increases as 1D flow rate increases and decreases as 2D flow rate increases. The influence of 1D- and 2D flow rate on 1D resolution observed within these factor ranges seems marginal, though. The oven temperature ramp appears to affect the 1D resolution a lot more.

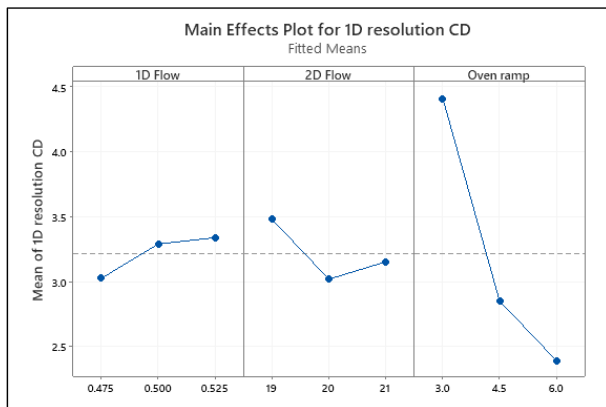


Figure 20: Main Effects plot for 1D resolution between C and D. Mean of resolution vs 1D flow rate, 2D flow rate and oven temperature ramp, from left to right (own work).

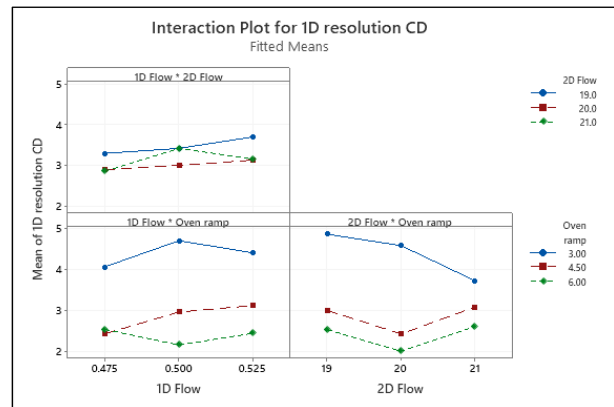


Figure 21: Interaction plot for 2D resolution between A and C. 1D- vs 2D flow rate on top left, 1D flow rate vs oven temperature ramp in bottom left, and 2D flow rate vs oven temperature ramp on the right (own work).

The separation in the primary column, which is mainly based on boiling point, benefits from a slower oven ramp. The interaction plot in figure 21 indicates that the 1D- and 2D flow rate affect 1D resolution independent of each other. There appears to be some interaction between 2D flow rate and oven temperature ramp, though. The resolution is decreasing when 2D flow rate is increased at an oven temperature ramp of 3°C/min, but is increasing when 2D flow rate is increased at an oven temperature rate of 4.5 and 6°C/min. This interaction might be due to differences in 1D/2D flow interactions within the modulator at different temperatures. But a clear explanation as to why this interaction occurs may be beyond the scope of this project.

3. Peak area component C

Main effects for the peak area of component C (figure 17) are plotted in figure 22. 1D flow rate, 2D flow rate and oven temperature ramp appear to all affect the peak area of component C. The relatively low acquisition rate of a single quad MS can explain the reduction of peak area with increased 2D flow rate. (Liu, J., 2018), (Ong & Marriott, 2002), (Shimadzu, 2012).

Peak area appears to increase as the oven temperature increases. This effect may be caused by both the narrowing of peaks and the limited MS acquisition rate. As the oven temperature increases, the analytes elute in narrower bands, which can also be said for a higher 1D flow rate. This results in more analyte being collected during each modulation and therefore a better detection (Liu, J., 2018).

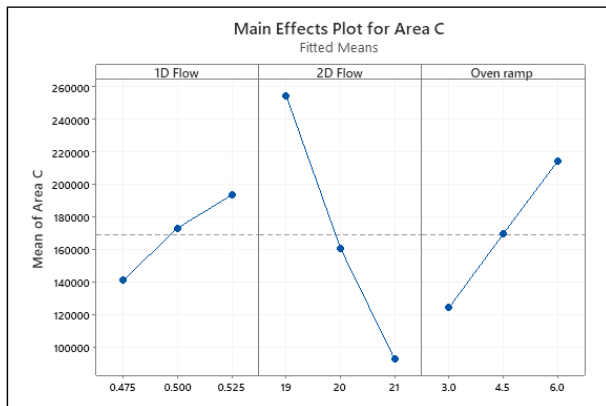


Figure 22: Main Effects plot for peak area C (counts•min). Mean of area vs 1D flow rate, 2D flow rate and oven temperature ramp, from left to right (own work).

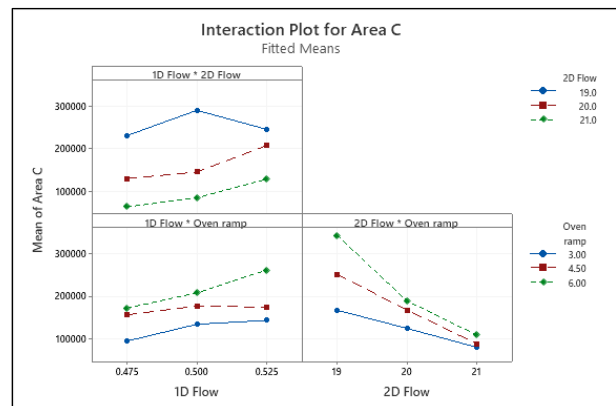


Figure 23: Interaction plot for 2D resolution between A and C. 1D- vs 2D flow rate on top left, 1D flow rate vs oven temperature ramp in bottom left, and 2D flow rate vs oven temperature ramp on the right (own work).

Overall, the following can be taken away from the DoE data discussed above: both the 1D- and 2D resolution appear to be high when a high 1D flow rate, a low 2D flow rate a low oven temperature ramp are applied. The peak area appears to be the highest with a high 1D flow rate, a low 2D flow rate and a high oven temperature ramp.

Selection of optimal parameter settings

An oven temperature ramp of 3°C/min favors the 1D- and 2D resolution, as indicated by the main effects plots in figures 18 and 20. The peak area is favored by an oven temperature ramp of 6°C/min, as indicated in figure 22. A compromised oven temperature ramp of 4.5°C/min was therefore selected for the general GCxGC method. But, a 3°C/min oven temperature ramp could be used for applications where resolution has priority, and a 6°C/min oven temperature ramp could be used for applications where peak area has priority.

It was initially considered to select 0.525 mL/min as the 1D flow rate and 19 mL/min as the 2D flow rate for the general GCxGC method. This combination of the highest 1D flow rate with the lowest 2D flow rate seemed obvious from the DoE data discussed above, and this combination was suggested as optimal in Minitab® as well. However, not all flow rate combinations applied during the DoE were confirmed to be compatible, as discussed in paragraph 4.1.1. The chromatogram resulting from applying the suggested flow rate combination showed streaking effects and it was therefore decided to select an alternative flow rate combination. Instead, a 1D flow rate of 0.525 mL/min and a 2D flow rate of 20 mL/min was selected to be used in the general GCxGC method. Streaking was not observed in the resulting chromatogram. The final parameter settings selected for the general GCxGC/MS method are listed in table 7.

Table 7: Optimal parameter settings for 1D flow rate (mL/min), 2D flow rate (mL/min) and oven temperature ramp (°C/min) for the general GCxGC/MS method.

Parameter	Setting
1D flow rate	0.525 mL/min
2D flow rate	20 mL/min
Oven temperature ramp	4.5°C

4.1.4 Repeatability of peak area

DAA 1 was analyzed in tenfold to determine the repeatability of the results generated by the developed GCxGC/MS method with regard to the amount of analyte detected. The area of compound C (figure 17) was recorded for each analysis and the RSD was calculated. The results are listed in appendix 11. The RSD of the area of compound C was 12.2%. There appears to be an overall downward trend in the peak area of compound C as the analysis number progresses. The downward trend is mainly caused by the areas of the first two analyses, which are relatively high. The trend in the data is further illustrated in figure 24, where the peak area of compound C is plotted against the analysis number. It is possible that the flow rate towards the MS is still too high, which may compromise the vacuum and functioning of the MS (Sudol et al., 2020).

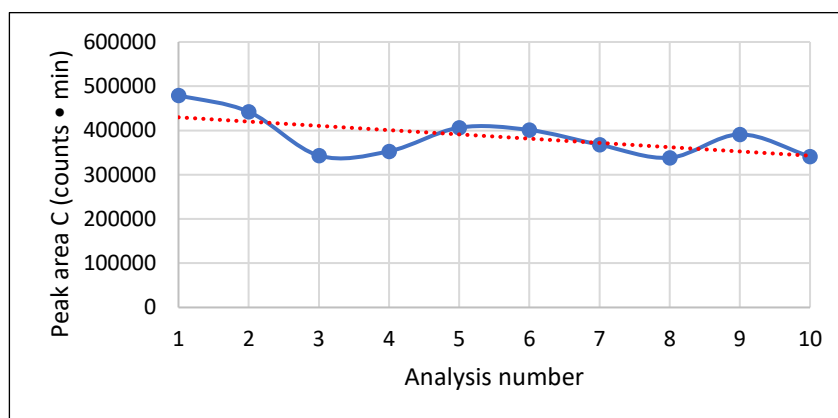


Figure 24: The area of compound C (counts • min) in DAA 1 plotted against the analysis number. The data was gathered using the developed GCxGC method (table 7).

Five analyses of DAA 1 were carried out using the developed GCxGC method in combination with FID. The RSD for the peak area of compound C in DAA 1 using FID as detector was 1.0%, which is much smaller than when the MS was used as detector. A total overview of the data is provided in appendix 12. There is a slight upward trend visible in the data. This is further illustrated in figure 25, where the peak area of compound C is plotted against the analysis number. The fact that the repeatability of peak area is better when an FID is used further indicates that it is likely that the root cause of poor repeatability after GCxGC/MS analysis lies with the MS.

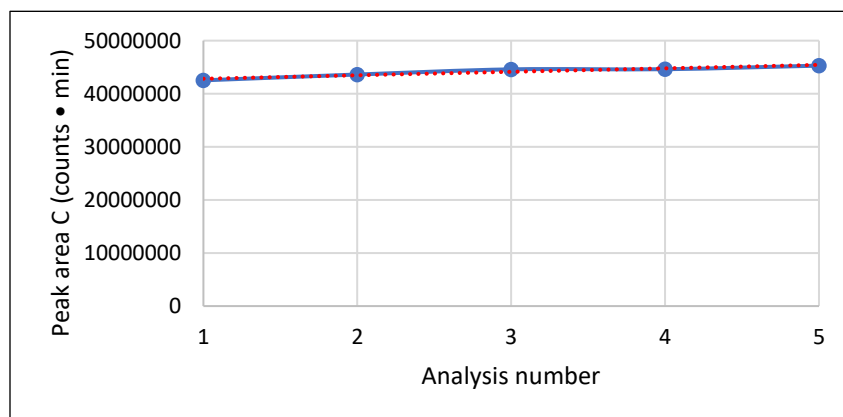


Figure 25: The area of compound C (counts • min) in DAA 1 plotted against the analysis number. The data was gathered using the developed GCxGC method (table 7).

4.1.5 Single column GC vs GCxGC

DAA 1 was analyzed with the single column GC/MS method currently applied at NXP and with the newly developed GCxGC/MS method (table 7). The results were compared with regard to compound separation and compound identification to determine the additional value of GCxGC compared to single column GC. A cut-out of the chromatogram resulting from the analysis of DAA 1 by single column GC is illustrated in appendix 13. The locations where compound identification was carried out are indicated by A, B, C and D in the single column GC chromatogram. A cut-out of the GCxGC chromatogram resulting from the analysis of DAA 1 is illustrated in 3D in figure 26 and in 2D in appendix 15. Peaks are indicated in GCxGC chromatograms by A, B, C and D. Full chromatograms are illustrated below each corresponding cut-out in appendix 14 and 16. The cut-out of the single column GC chromatogram shows three distinct peaks, whereas the GCxGC cut-outs show four distinct peaks. It appears therefore that GCxGC/MS analysis of DAAs is of additional value when it comes to separation of compounds.

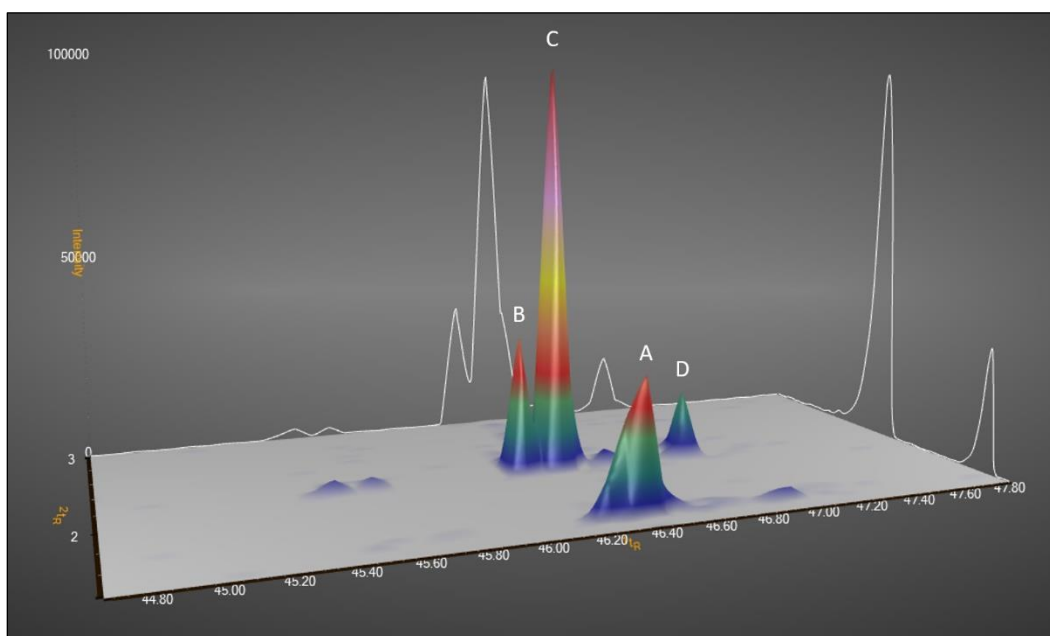


Figure 26: A 3D representation of a GCxGC chromatogram cut-out after analysis of DAA 1 with the developed method (Own work).

Normally, improved separation would lead to more reliable compound identification as well, but the additional value of GCxGC with regard to the reliability of compound identification is still questionable for the current GCxGC/MS set up. This is discussed in more detail below.

The results of compound identification in location A, B, C and D after single column GC/MS analysis of DAA 1 are listed in table 8. The compound name, identification score (%) and molecular structure are given. Four different compounds were identified with probabilities for A, B, C and D of 58%, 60%, 59%, and 62%, respectively.

Table 8: Identification of A, B, C and D (appendix 13) after analysis of DAA 1 by single column GC/MS. Listed are compound names, identification score (%) and molecular structure.

Compound	Name	Identification Score (%)	Molecular structure
A	4,7-Methano-1H-indene, 3a,4,7,7a-tetrahydro	58	
B	Pyrazolo[5,1-c]pyrido[2,3-e][1,2,4]-triazine-7-carbonitrile, 6,8-diamino-2-methyl	60	
C	4,7-Methano-1H-inden-6-ol, 3a,4,5,6,7,7a-hexahydro-, acetate	59	
D	Second isomer tricyclopentadiene	62	

Compound identification results for A, B, C and D after analysis of DAA 1 with the newly developed GCxGC/MS method are listed in table 9. Three different compounds were identified. B and D were identified as the same compound. The identification scores for A, B, C and D were 97%, 33%, 30% and 41%, respectively. The identification score of 97% for compound A is very high. The remaining three scores are low and these identifications can therefore not be regarded as reliable. The fact that compound B and D are similarly identified further underlines the unreliability of the results. B and D elute at different times and should be two different compounds. The MS spectra of compound B and D illustrated in appendices 17 and 18 are admittedly similar in many respects, but there are also differences. Furthermore, two entirely different compounds were identified for C after single column GC/MS and GCxGC/MS, as shown in table 8 and 9. The obtained mass spectra in these locations appear to be different in some respects, but they also show general similarities, as illustrated in appendix 19 and 20. This indicates that the operation of MS identification in combination with GCxGC requires further optimization.

Table 9: Identification of compound A, B, C and D (Figure 26 & appendix 15) after analysis of DAA1 with the newly developed GCxGC/MS method. Listed are compound names, probability (%) and molecular structure.

Compound	Name	Identification Score (%)	Molecular structure
A	4,9:5,8-Dimethano-1H-benzo[f]indene, 3a,4,4a,5,8,8a,9,9a-octrahydro-	97	
B	9-bromotricyclo[5.2.1.0(2,6)]dec-3-ene	33	
C	Tricyclo[6.2.1.0(2,7)]undec-9-ene, 4,5-divinyl	30	
D	9-bromotricyclo[5.2.1.0(2,6)]dec-3-ene	41	

4.2 PYR-GC/MS method development

Method development for PYR-GC/MS was carried out in two phases. First, evolved gas analysis (EGA) was carried out to determine the main decomposition temperatures of the materials in EMC 1, 2 and 3. The EGA data was used to select initial temperatures for pulsed pyrolysis and to select an end temperature for smart ramp pyrolysis. The influence of initial time settings on the results of pulsed pyrolysis was investigated in the second phase and an initial time was subsequently selected. The applicability of the chromatograms resulting from pulsed PYR-GC/MS analysis as fingerprints was determined by examining the amount of marker pyrolysates in each chromatogram and by determining repeatability. Smart ramp pyrolysis was carried out on EMC 1 and was carried out only once. Material characterization of EMCs by PYR-GC/MS was considered for both pulsed- and smart ramp pyrolysis

4.2.1 Pyrolysis temperatures from evolved gas analysis

An overlay of the EGA curves resulting from the analysis of EMC 1, 2 and 3 is illustrated in figure 27. The amount of evolved gas is set out against the acquisition time (min). The applied temperatures in the pyrolysis module were correlated to acquisition times based on the EGA temperature program (figure 10) and are displayed above the EGA curves in figure 27.

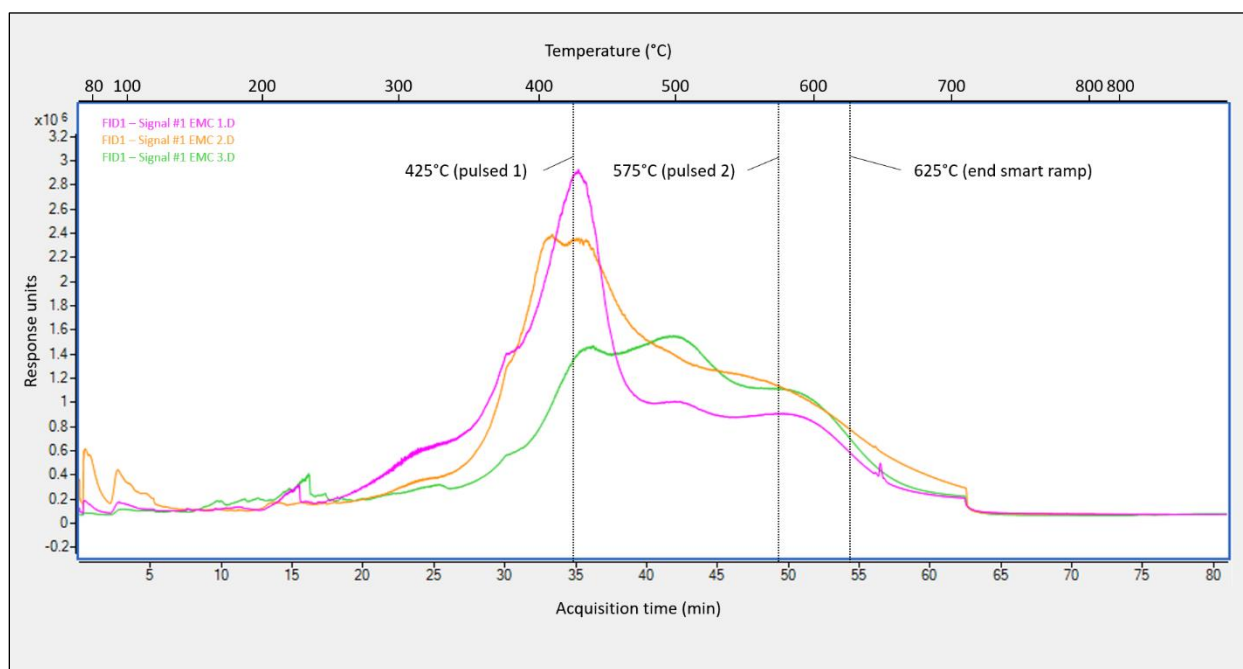


Figure 27: EGA curves for EMC 1, 2 and 3. Response units vs acquisition time (min) with correlating temperatures above the curves. 425°C is the first and 525°C is the second initial temperature selected for pulsed pyrolysis. 625°C is the selected end temperature for smart ramp pyrolysis (own work).

The analysis of EMC 1, 2 and 3 resulted in the three different EGA curves, highlighted in pink, orange and green, respectively. The amount of gas evolving from EMC 1 and 2 peaked just after 400°C. The amount of gas evolving from EMC 3 was also high around this temperature but experienced its maximum around 500°C. Response started to decline for EMC 1 and 3 around 600°C and around 525°C for EMC 2. Based on the EGA data displayed in figure 27, it was decided to select two initial temperatures for pulsed pyrolysis. The first initial temperature was calculated by averaging the temperatures at which the first peak in response was observed for each EMC. Here, pyrolysis of constituents with a relatively low decomposition

temperature took place. The second initial temperature was calculated by averaging the temperature at which the final decline in response set in for each EMC. During this phase, more thermally stable polymeric materials were decomposed. The first initial temperature for pulsed pyrolysis was set at 425°C and the second was set at 575°C. The end temperature for smart ramp pyrolysis was set at 625°C, 50°C above the temperature at which the last peak in response was observed for all three EMCs.

4.2.2 Selection of initial times

EMC 1 was analyzed by pulsed PYR-GC/MS with the initial temperatures set as discussed in paragraph 4.2.1. Initial times of 12, 18 and 24 seconds were applied. The resulting chromatograms were very similar to each other. MS data indicated that the identified compounds were similar for each initial time as well. An initial time of 12 seconds was therefore used during further analyses, as a longer initial time did not appear to have additional value. The initial time for smart ramp pyrolysis was also set at 12 seconds.

An overview of the pyrolysis temperatures and initial time selected for pulsed- and smart ramp PYR-GC/MS as discussed in paragraph 4.2.1 and 4.2.2 is provided in table 10.

Table 10: An overview of the pyrolysis temperatures and initial times selected for both pulsed- and smart ramp pyrolysis. Initial temperatures 1 and 2 for pulsed PYR-GC/MS and end temperature for smart ramp PYR-GC/MS.

Pyrolysis method	Pyrolysis temperatures	Initial time (sec)
Pulsed PYR-GC/MS	Initial 1: 425°C	12
	Initial 2: 575°C	12
Smart ramp PYR-GC/MS	End: 625°C	12

4.2.3 Pulsed PYR-GC/MS for EMC fingerprinting

EMC 1, 2 and 3 were analyzed by pulsed PYR-GC/MS with the selected initial temperatures and initial times. Initially, the chromatograms showed shifts in retention time and broad peaks for the more volatile compounds, such as benzene and toluene. Blank analysis after sample analysis also indicated that several less volatile compounds were not completely desorbed from the CIS. To solve these problems, it was decided to decrease the CIS initial temperature from -50°C to -150°C, to improve trapping of the volatile compounds, and to increase the CIS end temperature from 280°C to 350°C, to facilitate sufficient desorption from the CIS. After this, the volatile compounds were detected in reproduceable, sharp peaks and the blanks after sample analysis were clean. The optimized CIS settings are included in appendix 21, where the parameter settings for PYR-GC/MS are listed.

The chromatograms resulting from pulsed PYR-GC/MS analysis of EMC 1, 2 and 3 are illustrated in appendices 22, 23 and 24, respectively. Retention times of the pyrolysates and the intensities of the peaks are very much different in each of the three chromatograms. This favors their applicability as fingerprints, as these fingerprints should be unique for each material. Compound identification based on the MS data also shows that the fingerprints generated are very much different between each EMC. In each chromatogram, twelve of the twenty highest peaks could be identified as marker pyrolysates. These marker pyrolysates are compounds that are unique for each EMC within the examined set and contribute to the applicability of the chromatograms as fingerprints. The peaks of the marker pyrolysates for EMC 1,

2 and 3 are indicated with arrows in appendix 22, 23 and 24, respectively. The remaining eight of the twenty highest peaks were attributed to more volatile constituents and pyrolysates identified for each of the three EMCs. These include propene, acetone, benzene, toluene, ethylbenzene, p-xylene, phenol and 2-methyl-phenol.

EMC 1 was analyzed in triplo to determine the repeatability of the results. An overlay of the three resulting chromatograms is illustrated in figure 28. It was demonstrated in several ways that these chromatograms are extremely similar to each other. A cut-out of the chromatogram in the time frame of 33-35 minutes is provided in figure 28 as well. This cut-out shows the similarities between the chromatograms in the section where these are less obvious.

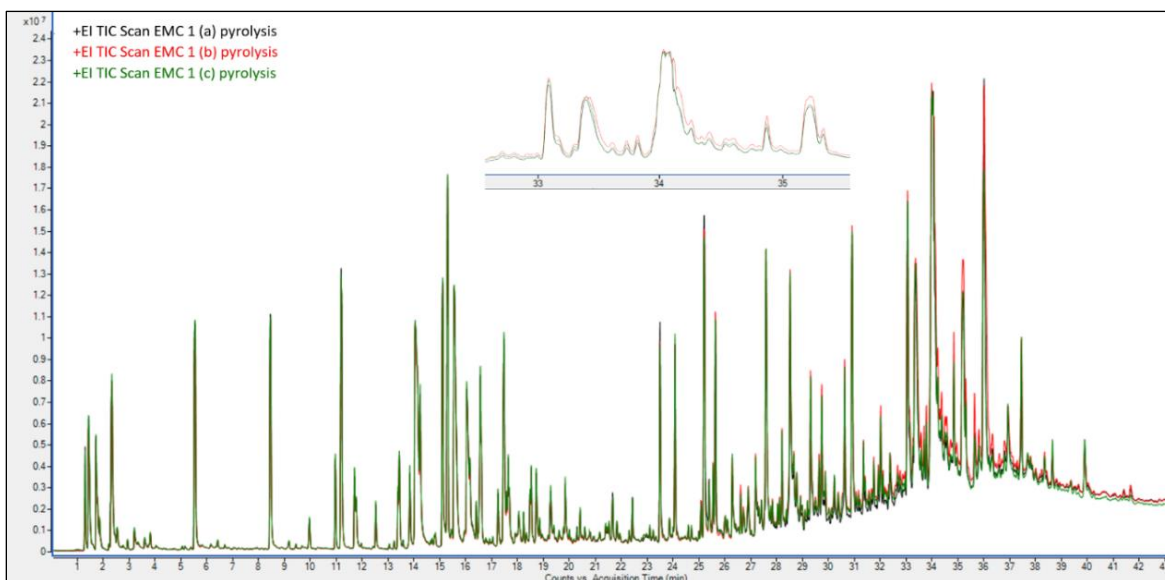


Figure 28: An overlay of the PYR-GC/MS chromatograms for triplo analysis of EMC 1. Pyrolysis was carried out in pulsed mode with initial temperatures 425°C and 575°C, and an initial time of 12 seconds (own work).

Compound identification was carried out for the twenty highest peaks of each chromatogram in figure 28. The identified compounds were identical for each chromatogram and are listed in appendices 24 and 25. The repeatability of relative peak heights in triplo was determined and resulted in an average RSD of 3.89% (appendix 26). Repeatability of retention times was excellent with an average RSD of 0.05% (appendix 27). These results for the repeatability of relative peak heights and retention times are strong indications that PYR-GC/MS analysis with the selected settings can be used to generate chromatograms that can serve as fingerprints.

4.2.4 PYR-GC/MS for material characterization

Besides the generation of fingerprints, PYR-GC/MS can be applied to gain insight into the chemical composition of materials. The specific set of pyrolysates generated can be traced back to the composition of the original sample. The characterization of polymers and certain additives in EMCs may be possible by PYR-GC/MS. A tentative indication of the possibilities in terms of material characterization by PYR-GC/MS is provided below.

Ideally, a database with pyrolysis chromatograms of pure polymeric materials and additives is used to determine the composition of EMCs. An indication of their composition can be given, though. The set of marker pyrolysates for EMC 1 contains several bi-phenylic and di-phenylic compounds. Examples of these compounds are illustrated in figure 29. Comparing the compounds in figure 29 to the polymers illustrated in figure 2 indicates that a multi aromatic or biphenyl type epoxy resin was used in EMC 1. The marker pyrolysates of EMC 2 illustrated in figure 30 indicate that the use of a multi aromatic resin is very likely. The set of marker pyrolysates for EMC 3 is characterized by a variety of phenolic compounds, as illustrated in figure 31. A Novolac type epoxy resin is the most likely candidate for EMC 3 when comparing these compounds with the polymers in figure 2. The findings of these analyses match to a certain extent with what is known about EMC 1-3 (table 2), which is promising for future application of PYR-GC/MS for material characterization.

Pulsed PYR-GC/MS has also proven to be useful in distinguishing between high-sulfur and non-sulfurous variants of EMC 2. The component *2,5-dihydrothiophene sulfone* was detected after analysis of the high-sulfur variant, and no sulfurous components were detected after analysis of the non-sulfurous variant. Several raw materials commonly present in EMCs listed in table 1 have been identified as well. Examples of these components with their corresponding function are listed in table 11.

Table 11: Examples of components identified by pulsed PYR-GC/MS with their corresponding function in EMCs. Theoretical examples of raw materials commonly present in EMCs are listed in table 1.

Component	Function in EMCs
Cyclotrisiloxane, hexamethyl	Low stress additive
Cyclotrisiloxane, octamethyl	Low stress additive
Triphenylphosphine oxide	Catalyst
Amino silane	Coupling agent

A single smart ramp PYR-GC/MS analysis of EMC 1 was carried out and resulted in the chromatogram illustrated in appendix 25. This chromatogram appears to be different to that resulting from pulsed PYR-GC/MS analysis of EMC 1. The temperature program in smart ramp pyrolysis (figure 12) covers the optimal pyrolysis temperatures of all constituents in EMCs, which might result in more realistic chemical information in the chromatograms. It may therefore be interesting to further investigate the application of smart ramp pyrolysis for material characterization of EMCs.

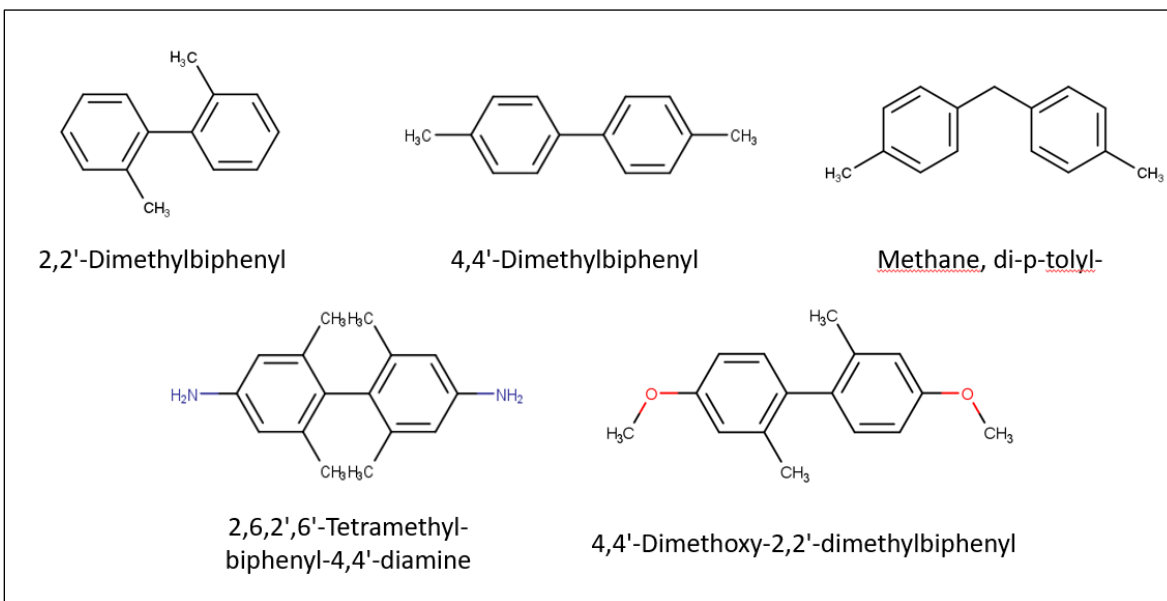


Figure 29: The chemical structures with corresponding IUPAC names of five marker pyrolysates identified in EMC1 after analysis with pulsed PYR-GC/MS.

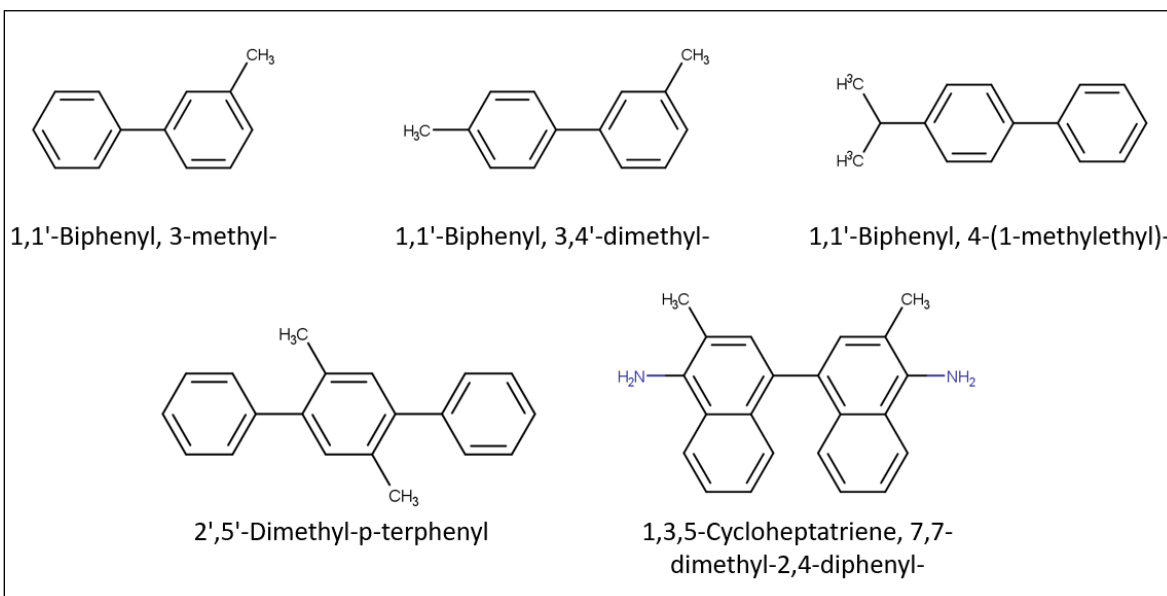


Figure 30: The chemical structures with corresponding IUPAC names of five marker pyrolysates identified in EMC 2 after analysis with pulsed PYR-GC/MS.

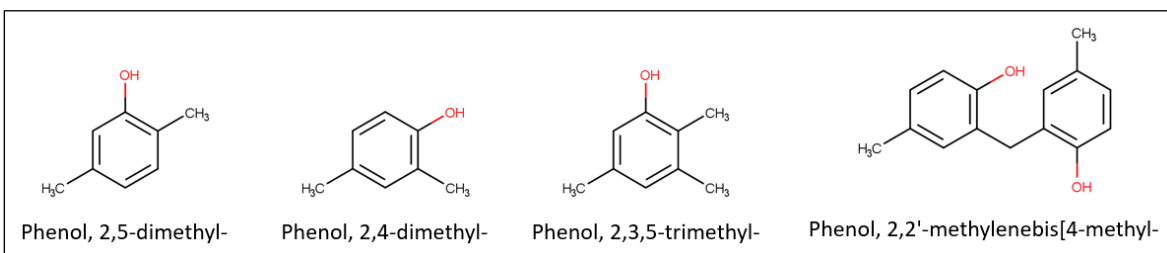


Figure 31: The chemical structures with corresponding IUPAC names of five marker pyrolysates identified in EMC 3 after analysis with pulsed PYR-GC/MS.

5. Discussion

Method development for GCxGC/MS and PYR-GC/MS has been carried out in two separate projects. The implications, applications and limitations of the results are discussed in this chapter. The results of GCxGC project will be discussed first, followed by the results of the pyrolysis project.

5.1 GCxGC/MS

The goal concerning GCxGC consisted of two parts. First, a method had to be developed in which GCxGC parameter settings were optimized to maximize both separation and detection of VOCs in DAAs. After that, the additional value of GCxGC analysis compared to the traditionally applied single column GC analysis had to be assessed with regard to compound separation and compound identification. GCxGC/MS method development was realized by first determining the operating window of flow rates and then optimize settings for 1D flow rate, 2D flow rate and oven temperature ramp to maximize 1D resolution, 2D resolution and peak area.

The operating window is defined during the GCxGC project as the set of compatible 1D- and 2D flow rates. The scope of the operating window was determined to reduce the likelihood that undesirable chromatographic effects were encountered during further method development. The final operating window and the effects that limit its scope are illustrated in the diagram in figure 15. The compatibility of flow rates surrounding a 1D flow rate of around 0.5 mL/min and a 2D flow rate of around 20 mL/min was expected based on the advice of the supplier. The resulting operating window matches this expectation. Streaking and absence of peaks were both expected to be encountered as undesirable effects, but it was not expected prior to the experimental phase that MS fouling and lack of 2D retention would occur. The determination of the GCxGC operating window served as a preliminary phase to the optimization of flow rates and oven temperature ramp by means of Experimental Design. It gave an indication which flow rate combinations should be avoided, which was of great importance for the proper execution of the DoE. It is important to note that the operating window has a 'limited resolution', so to speak. It only gives information about the compatibility of the flow rates that were investigated. The compatibility of, for example, a 1D flow rate of 0.525 mL/min with a 2D flow rate of 19 mL/min cannot be derived from it. This meant that not all the flow rate combinations applied during the DoE could be confirmed to be free of undesirable effects based on the operating window.

The parameter settings for 1D flow rate, 2D flow rate and oven temperature ramp were optimized to maximize 1D resolution, 2D resolution and peak area. This was realized by means of Experimental Design. A 1D flow rate of 0.525 mL/min, a 2D flow rate of 20 mL/min and a oven temperature ramp of 4.5°C/min were selected as parameter settings for the general GCxGC/MS method. Both 1D and 2D resolution seemed to benefit from a high 1D flow rate, a low 2D flow rate and a low oven temperature ramp. The peak area was the highest when 1D flow rate was high, 2D flow rate was low and oven temperature was high. The optimal flow rates are very specific to the GCxGC set-up used, as a wide variety of column dimensions is available. Optimal settings within these ranges were expected, though, based on information given by the supplier. The effects of the oven temperature ramp illustrated in figure 18, 20 and 22 lead to the selection of a compromised temperature ramp for the general GCxGC/MS method. This compromise is also reported in other research (Liu, J., 2018).

A limitation of the DoE data analysis is that the significance of the effects and interactions was not statistically substantiated. The effects of factors and interactions between factors were judged relative to each other. However, the observed effects would probably lead to the selection of the same parameter settings, regardless of their significance. Furthermore, the poor repeatability of GCxGC/MS peak area may have negatively affected the quality of the DoE. Further research on effects of factors and the interactions between them may therefore be necessary. GCxGC/MS method development was also limited due to the use of a specific DAA sample. Broader applicability of the method has not been demonstrated. It is therefore recommended to determine the applicability of the method by analyzing a wider variety of samples. VOCs can for example be desorbed from EMCs and subsequently analyzed by GCxGC/MS.

The GCxGC/MS method was developed to generate data that could be compared to data acquired by single column GC/MS with regard to compound separation and compound identification. It was expected that GCxGC/MS analysis would result in both improved separation and improved compound identification, as the superiority of GCxGC is reported in several studies regarding these items (Liu, J., 2018), (Mostafa et al., 2012), (Ong & Marriott, 2002), (Shimadzu, 2012), (Winnike et al., 2015). Analysis of DAA with the developed GCxGC/MS method showed that the separation of compounds does indeed benefit from analysis in two dimensions. Compounds that were not separated by single column GC/MS (appendix 13) were separated by GCxGC/MS (appendix 15). However, the identification of compounds in the GCxGC chromatograms was largely unreliable, as indicated in table 8 and 9. Repeatability of peak area was poor as well (appendix 11). This indicates that the current application of GCxGC/MS needs further optimization when it comes to repeatability and compound identification.

A solution must be found for the poor repeatability of GCxGC results. Gradual decrease in detection by the MS may indicate that the split flow to the MS is too high. Especially because the repeatability of the results is good when an FID is used as detector (appendix 12). The effluent split from the secondary column to MS:FID currently varies between 1:8 and 1:5. With a 2D flow rate of 20 mL/min, flow rates of between 2.5 and 4.0 mL/min are directed toward the MS, which may lead to temporary fouling. It is possible that this effect contributes to decrease in sensitivity and poor repeatability (Rood, 1998). A compromised vacuum due to the high flow rates may also contribute (Sudol et al., 2020). Results of PYR-GC/MS analyses show that repeatable results can be generated when the flow rate to the MS is 1.2 mL/min. The effect of using transfer lines with alternative dimensions to lower the flow to the MS should therefore be investigated. The transfer line to the MS should be longer or have a narrower bore to shift the split in favor of the FID. It is also possible to use a transfer line to the FID that is shorter or has a wider bore compared to the currently used transfer line.

Normally, detectors such as TOF-MS or FID are used in combination with GCxGC, because of their high acquisition rate. The acquisition rate applied in the single quadrupole MS was 4.4 Hz, which is relatively low. This makes it less compatible with the high eluent flow in the secondary column (Mostafa et al., 2012), (Ong & Marriott, 2002), (Shimadzu, 2012). It is possible that a higher acquisition rate can be applied on the new system. This may lead to more repeatable results, and should therefore be investigated. The poor results for compound identification may also be caused by the low acquisition rate. But it is also possible that the cause lies with the identification tool and database, because two entirely different compounds were identified for C after GC and GCxGC analysis. The mass spectra of C do show differences, but also general similarities (appendices 19 & 20).

5.2 PYR-GC/MS

The goal concerning the pyrolysis option was to create a PYR-GC/MS method that can generate EMC fingerprints and would allow for an initial exploration of the capabilities of PYR-GC/MS in terms of material characterization of EMCs. Pyrolysis temperatures were selected based on EGA data, after which the required initial time was selected. The applications of pulsed PYR-GC/MS for EMC fingerprinting were subsequently examined, as well as the application of pulsed- and smart ramp PYR-GC/MS for material characterization.

EGA was carried out to determine the main decomposition temperatures in EMCs. The optimal initial temperatures for pulsed PYR-GC/MS and the end temperature for smart ramp PYR-GC/MS were expected to be dependent on the decomposition temperatures of the EMCs (Ma et al., 2014). Which temperatures that could be was entirely unknown. The initial temperatures selected for pulsed PYR-GC/MS based on the EGA data were 425°C and 575°C. The selected end temperature for smart ramp pyrolysis was 625°C. Initial times were set at 12 seconds for both pulsed- and smart ramp pyrolysis, because the application of 12, 18 and 24 seconds as initial times resulted in similar chromatograms. The determination of settings for pyrolysis temperatures and pyrolysis duration enabled the application of pulsed- and smart ramp PYR-GC/MS analysis of EMCs.

Several comments can be made on the selection of pyrolysis temperatures. First of all, the initial temperatures selected for pulsed PYR-GC/MS are compromised temperatures. They are averages of decomposition temperatures of three different EMCs. It is likely that the selected temperatures are therefore not optimal for each EMCs. Moreover, EMCs are not composed of one pure material, which is why the initial temperatures that were selected are also likely to be less than optimal for a selection of the components present in EMCs. The end temperature for smart ramp pyrolysis of 625°C could be disputed as well. The selected temperature is 50°C above the second initial temperature of pulsed PYR-GC/MS, but it is the question if this temperature is high enough. Some components in the EMCs may pyrolyze at a higher temperature. The effect of applying higher end temperatures during smart ramp PYR-GC/MS could be investigated during future research.

The applicability of chromatograms generated by pulsed PYR-GC/MS analysis of EMCs as fingerprints was examined after the selection of initial temperatures and an initial time. The chromatograms resulting from the analysis of three different EMCs differed from each other in that twelve of the twenty largest peaks could be identified as marker pyrolysates in each of the three chromatograms. Triplo analysis of EMC 1 resulted in average RSDs for retention time and relative peak height of 3.89% and 0.05%, respectively. If pulsed PYR-GC/MS analysis of EMCs would result in significantly different chromatograms was entirely unknown prior to the experiments. The excellent repeatability of pulsed PYR-GC/MS is reported, though (Kleine Benne, E. & Zhou, H. X., Gerstel GmbH & Co. KG, video lecture on pyrolysis).

The results indicate that pulsed PYR-GC/MS can indeed be applied to generate EMC fingerprints. There are several applications possible for EMC fingerprinting. These include quality control and analysis of competitor materials. Fingerprint matching may for example be of use for quality control when a possible mix-up of EMC batches must be investigated. Possible effects of changes in production processes of EMCs can be investigated as well. PYR-GC/MS analysis of EMCs of competitors may indicate to what degree these differ from the EMCs that NXP uses.

The method used to determine if the chromatograms contained marker pyrolysates has its limits as well. The presence of marker pyrolysates was determined based only on the twenty highest peaks. It is therefore possible that a component identified as marker pyrolysate was also present in one of the other chromatograms, but in an amount sufficiently low to be excluded from the twenty highest peaks. An examination of all the components identified after pulsed PYR-GC/MS analysis of EMCs should be carried out to determine which compounds are true markers for each EMC. Also, more EMCs should be analyzed in future research to further expand the fingerprint database.

A first insight into the possibilities in terms of material characterization by PYR-GC/MS was provided besides the examination fingerprinting applications. Several pyrolysates were identified that correctly indicate the polymeric materials present in each EMC (figure 29, 30, 31). There were also compounds identified that gave information about the types of additives present (table 11). These results are in line with the application of PYR-GC/MS for material characterization reported in literature (Kusch, 2017), (Rial-Otero et al., 2009). They also indicate that much more is possible when it comes to material characterization by PYR-GC/MS. The application of smart ramp pyrolysis for this purpose should for example be investigated further during future research. The chromatograms resulting from this could provide more realistic information, as the optimal pyrolysis temperatures for each constituent in the EMCs are included in the temperature program.

Finally, the capabilities of GCxGC and pyrolysis could be further investigated in future research by combining both techniques. Improved separation may be of use considering the complexity of the chromatograms resulting from PYR-GC/MS analysis of EMCs. PYR-GCxGC/MS analysis may provide improved fingerprinting capabilities and more extensive material characterization (Han et al., 2016).

6. Conclusions

Comprehensive multidimensional GC (GCxGC) and pyrolysis were introduced at NXP semiconductors after the acquisition of a new GC/MS system. NXP aims to explore the capabilities of GCxGC and pyrolysis by developing methods for both techniques to enhance the quality and extent of material analysis. Method development for GCxGC/MS and PYR-GC/MS, and subsequent evaluation of the capabilities of both techniques was therefore carried out in two separate projects. The conclusions following from the results gathered during both projects are presented in this chapter. Conclusion about GCxGC/MS will be presented first, followed by conclusions about PYR-GC/MS.

6.1 GCxGC/MS

The goals concerning GCxGC were to first develop a method in which GCxGC parameter settings were optimized to maximize both separation and detection of VOCs in DAAs, and then assess the additional value of GCxGC analysis compared to the traditionally applied single column GC analysis with regard to compound separation and compound identification. The GCxGC parameters settings for 1D flow rate, 2D flow rate and oven temperature ramp were therefore optimized to maximize 1D resolution, 2D resolution and peak area. The parameter meter settings selected for the general GCxGC/MS method based on DoE data were a 1D flow rate of 0.525 mL/min, a 2D flow rate of 20 mL/min and an oven temperature ramp of 4.5 mL/min. The goal of developing a GCxGC/MS method has therefore been achieved.

The additional value of GCxGC compared to single column GC was assessed by considering compound separation, compound identification and repeatability of peak area. GCxGC/MS analysis of DAA resulted in separation of compounds that were not separated by single column GC/MS. However, the repeatability of peak area was poor and compound identification results turned out to be largely unreliable. It was therefore concluded that the current application of GCxGC/MS at NXP provides additional value compared to the current single column GC/MS analysis with regard to compound separation, but needs further optimization when it comes to repeatability and compound identification.

6.2 PYR-GC/MS

The goal concerning the pyrolysis option was to create a PYR-GC/MS method that can generate EMC fingerprints and would allow for an initial exploration of the capabilities of PYR-GC/MS in terms of material characterization. Initial temperatures and initial times were therefore selected to enable the application of pulsed PYR-GC/MS for these purposes. An end temperature and initial time for smart ramp pyrolysis were selected to enable a comparison between pulsed- and smart ramp pyrolysis regarding their application in material characterization. The initial temperatures selected for pulsed PYR-GC/MS are 425°C and 575°C. The end temperature selected for smart ramp PYR-GC/MS is 625°C. Initial times were set at 12 seconds for both pulsed- and smart ramp pyrolysis.

The chromatograms resulting from pulsed PYR-GC/MS analysis of the EMCs contained marker pyrolysates that made it possible to distinguish between different EMCs based on the data. Repeatability of both relative peak height and retention time were excellent. It can therefore be concluded that the developed PYR-GC/MS method can be used to generate EMC fingerprints.

The application of pulsed PYR-GC/MS regarding material characterization was explored by examining the pyrolysates that were identified for each EMC. The types of pyrolysates identified indicated the presence



of certain raw materials in the EMCs, such as polymers and several additives. Smart ramp PYR-GC/MS analysis of EMC also showed promising results. The application of both pulsed- and smart ramp pyrolysis should therefore be considered during further research on the application of PYR-GC/MS for material characterization.

7. Bibliography

- Agilent Technologies, Inc. (2007). *Agilent Capillary Flow Technology Simpler, more reliable GC x GC*. Agilent. Retrieved March 2, 2022, from https://www.agilent.com/cs/library/brochures/5989_7631EN_HiResCMYK.pdf
- Cordero, C., Rubiolo, P., Sgorbini, B., Galli, M., & Bicchi, C. (2006). Comprehensive two-dimensional gas chromatography in the analysis of volatile samples of natural origin: A multidisciplinary approach to evaluate the influence of second dimension column coated with mixed stationary phases on system orthogonality. *Journal of Chromatography A*, 1132(1–2), 268–279. <https://doi.org/10.1016/j.chroma.2006.07.067>
- Dömötöróvá, M., Kirchner, M., Matisová, E., & De Zeeuw, J. (2006). Possibilities and limitations of fast GC with narrow-bore columns. *Journal of Separation Science*, 29(8), 1051–1063. <https://doi.org/10.1002/jssc.200500472>
- Duhamel, C., Cardinael, P., Peulon-Agasse, V., Firor, R., Pascaud, L., Semard-Jousset, G., Giusti, P., & Livadaris, V. (2015b). Comparison of cryogenic and differential flow (forward and reverse fill/flush) modulators and applications to the analysis of heavy petroleum cuts by high-temperature comprehensive gas chromatography. *Journal of Chromatography A*, 1387, 95–103. <https://doi.org/10.1016/j.chroma.2015.01.095>
- Fan, L. (2015, March 19). *Epoxy molding compound, its manufacturing process and use, and transistor outline package product containing molded product thereof*. Patents.Google.Com. Retrieved March 1, 2022, from <https://patents.google.com/patent/WO2016145661A1/en>
- Gerstel GmbH & Co. KG. (2011, March). *Versatile Automated Pyrolysis GC Combining a Filament Type Pyrolyzer with a Thermal Desorption Unit*. <https://www.gerstelus.com/>. Retrieved May 12, 2022, from https://www.gerstelus.com/wp-content/uploads/2017/07/2011-04_pyrolysis-overview.pdf
- GERSTEL GmbH & Co.KG. (2022). *Pyrolysis | GERSTEL*. <https://www-prod.gerstel.com>. Retrieved February 15, 2022, from <https://www-prod.gerstel.com/en/Pyrolysis>
- GERSTEL Inc. (2018, 13 november). *Thermal Desorption Unit - TDU*. www.gerstelus.com. Retrieved April 11, 2022, from <https://www.gerstelus.com/product/tdu/>
- Gotro, J. (2017, June 5). *Polymers in Electronics Part Eight: Die Attach Adhesives Part 1*. Polymer Innovation Blog. Retrieved April 7, 2022, from <https://polymerinnovationblog.com/polymers-electronics-part-eight-die-attach-adhesives-part-1/>
- Griffith, J. F., Winniford, W. L., Sun, K., Edam, R., & Luong, J. C. (2012). A reversed-flow differential flow modulator for comprehensive two-dimensional gas chromatography. *Journal of Chromatography A*, 1226, 116–123. <https://doi.org/10.1016/j.chroma.2011.11.036>
- Han, B., Daheur, G., & Sablier, M. (2016). Py-GC×GC/MS in cultural heritage studies: An illustration through analytical characterization of traditional East Asian handmade papers. *Journal of Analytical and Applied Pyrolysis*, 122, 458–467. <https://doi.org/10.1016/j.jaap.2016.10.018>
- Harris, D. C. (2016). *Quantitative Chemical Analysis [May 29, 2015] Harris, Daniel C.* (9th ed., Vol. 3). WH Freeman. Chapter 24, Gas Chromatography, Pages 633-662
- Harynuk, J., Górecki, T., & Zeeuw, J. D. (2005). Overloading of the second-dimension column in comprehensive two-dimensional gas chromatography. *Journal of Chromatography A*, 1071(1–2), 21–27. <https://doi.org/10.1016/j.chroma.2004.11.049>
- JSB. (n.d.). *OUR GC×GC MODULATORS: AN OVERVIEW*. [Go-Jsb.Com](http://www.go-jsb.com). Retrieved February 28, 2022, from https://www.go-jsb.com/resources/media/GCxGC_Modulator_overview.pdf
- Kusch, P. (2017). Application of Pyrolysis-Gas Chromatography/Mass Spectrometry (Py-GC/MS). *Characterization and Analysis of Microplastics*, 75, 169–207. <https://doi.org/10.1016/bs.coac.2016.10.003>
- Lai, Y. L., & Ho, C. Y. (2004). Electrical modeling of quad flat no-lead packages for high-frequency IC applications. *2004 IEEE Region 10 Conference TENCON 2004.*, 344–347. <https://doi.org/10.1109/tencon.2004.1414940>
- LECO Empowering Results. (n.d.). *GC×GC : Comprehensive Two-Dimensional Gas Chromatography*. Leco.Com. Retrieved March 2, 2022, from <https://www.leco.com/gcxgc#:~:text=Research%20has%20shown%20the%20benefits,plots%2C%20and%20sensitivity%20enhancement>.
- Libretexts. (2020, 11 augustus). *12.4: Gas Chromatography*. Chemistry LibreTexts. Retrieved on May 8, 2022, from https://chem.libretexts.org/Courses/Northeastern_University/12%3A_Chromatographic_and_Electrophoretic_Methods/12.4%3A_Gas_Chromatography
- Liu, J. (2018). *Development and Applications of Functionalized Octatetrayne as Novel Carbon Media in Chromatography*. The Ohio State University ProQuest Dissertations Publishing. Retrieved May 28, 2022, from https://etd.ohiolink.edu/apexprod/rws_olink/r/1501/10?clear=10&p10_accession_num=osu1519322396476316

- Ma, X. M., Lu, R., & Miyakoshi, T. (2014). Application of Pyrolysis Gas Chromatography/Mass Spectrometry in Lacquer Research: A Review. *Polymers*, 6(1), 132–144. <https://doi.org/10.3390/polym6010132>
- Mettler-Toledo International Inc. (2020, December 1). *Webinar – Thermal Analysis of Thermosets*. Mettler-Toledo International Inc. all rights reserved. Retrieved February 11, 2022, from https://www.mt.com/be/fr/home/library/on-demand-webinars/lab-analytical-instruments/Thermal_Analysis_of_Thermosets.html
- Mostafa, A., Edwards, M., & Górecki, T. (2012). Optimization aspects of comprehensive two-dimensional gas chromatography. *Journal of Chromatography A*, 1255, 38–55. <https://doi.org/10.1016/j.chroma.2012.02.064>
- NXP Semiconductors. (2022, January 31). *About NXP*. Nxp.Com. Retrieved February 10, 2022, from <https://www.nxp.com/company/about-nxp:ABOUT-NXP>
- Omais, B., Courtiade, M., Charon, N., Ponthus, J., & Thiébaud, D. (2011). Considerations on Orthogonality Duality in Comprehensive Two-Dimensional Gas Chromatography. *Analytical Chemistry*, 83(19), 7550–7554. <https://doi.org/10.1021/ac201103e>
- Ong, R. C. Y., & Marriott, P. J. (2002). A Review of Basic Concepts in Comprehensive Two-Dimensional Gas Chromatography. *Journal of Chromatographic Science*, 40(5), 276–291. <https://doi.org/10.1093/chromsci/40.5.276>
- Sudol, P. E., Pierce, K. M., Prebihalo, S. E., Skogerboe, K. J., Wright, B. W., & Synovec, R. E. (2020). Development of gas chromatographic pattern recognition and classification tools for compliance and forensic analyses of fuels: A review. *Analytica Chimica Acta*, 1132, 157–186. <https://doi.org/10.1016/j.aca.2020.07.027>
- Procter, P. (n.d.). *Mold Compound | Semiconductor Digest*. Semiconductor-Digest.Com. Retrieved March 1, 2022, from <https://sst.semiconductor-digest.com/2003/10/mold-compound/>
- Restek. (2012). *GCxGC Columns Your One Source for 2D Gas Chromatography*. restek.com. Retrieved May 6, 2022, from <https://www.restek.com/globalassets/pdfs/literature/gnbr1585-unv.pdf?id=1611870280238/>
- Restek. (2022). *Restek GCxGC Column Combination Guide*. Restek.Com. Retrieved May 6 2022, from <https://www.restek.com/row/technical-literature-library/articles/restek-GCxGC-column-combination-guide/>
- Rial-Otero, R., Galesio, M., Capelo, J. L., & Simal-Gándara, J. (2009). A Review of Synthetic Polymer Characterization by Pyrolysis–GC–MS. *Chromatographia*, 70(3–4), 339–348. <https://doi.org/10.1365/s10337-009-1254-1>
- Rood, D. (1998). Gas Chromatography Problem Solving and Troubleshooting. *Journal of Chromatographic Science*, 36(5), 275. <https://doi.org/10.1093/chromsci/36.5.275>
- SGE Analytical Science. (n.d.). *GC Capillary Columns*. www.duratec.info. Retrieved May 6 2022, from https://www.duratec.info/index.php?option=com_docman&task=doc_view&gid=107&Itemid=10&lang=de
- Shimadzu. (2012). *GCxGC Handbook - Fundamental Principles of Comprehensive 2D GC (C146-E177)*. Shimadzu. Retrieved March 4, 2022, from <https://www.an.shimadzu.co.jp/gcms/gcxgc/c146-e177.pdf>
- SRA Instruments. (2021, July 29). *Thermal Desorption Unit TDU 2*. <https://www.srainstruments.com/>. Retrieved March 3, 2022, from <https://www.srainstruments.com/p/tdu/>
- Stuff, J. R., Whitecavage, J. A., McAdams, M., Nie, Y., & Kleine-Benne, E. (2012). *GERSTEL AppNote Nr. 159 - Thermal Gravimetric Analysis/Mass Spectrometry Simulation using the GERSTEL Automated Pyrolyzer*. Gerstel GmbH & Co. KG. Retrieved March 7, 2022, from <http://ch.gerstel.com/pdf/p-gc-an-2012-14.pdf>
- Sasajima, H., Watanabe, I., Takamoto, M., Dakede, K., Itoh, S., Nishitani, Y., Tabei, J., & Mori, T. (2016). New Development Trend of Epoxy Molding Compound for Encapsulating Semiconductor Chips. *Materials for Advanced Packaging*, 373–419. https://doi.org/10.1007/978-3-319-45098-8_9
- Sumitomo Bakelite Co., Ltd. (2015). *Epoxy Resin Molding Compounds for Encapsulation of Semiconductor Devices SUMICON (R) EME | Sumitomo Bakelite Co., Ltd.* Sumibe.Co.Jp/English/. Retrieved March 1, 2022, from <https://www.sumibe.co.jp/english/product/it-materials/epoxy/sumikon-eme/>
- Winnike, J. H., Wei, X., Knagge, K. J., Colman, S. D., Gregory, S. G., & Zhang, X. (2015). Comparison of GC-MS and GC×GC-MS in the Analysis of Human Serum Samples for Biomarker Discovery. *Journal of Proteome Research*, 14(4), 1810–1817. <https://doi.org/10.1021/pr5011923>
- Woodward, Z. (March 12, 2020). *How Phase Ratio Can Shorten Run-times While Preserving Resolution*. Phenomenex.Com. Retrieved May 7 2022, from <https://phenomenex.blog/2020/03/12/phase-ratio/#:%7E:text=Phase%20ratio%20represents%20the%20dynamic,used%20for%20your%20initial%20method.>

8. Appendices

Appendix 1: An overview of the general settings applying to liquid injection GC/MS when using the traditional single column GC/MS on the old GC system.

Process	Parameter	Setting
GC	Column	J&W VF-1ms, 30 m, 0.25 mm I.D., 1.00 µm D _f , 100% Dimethylpolysiloxane
	Injector temperature	300°C
	Carrier gas	Helium
	Flow rate	1.2 mL/min
Oven	Oven initial temperature	40°C
	Oven ramp 1	8°C/min to 110°C, 0 min hold
	Oven ramp 2	10°C/min to 300°C, 15.25 min hold
	Oven end temperature	300°C
	Run time	45 min
MS	Mass range	29-350 amu
	Acquisition rate	4.4 Hz
Liquid injection	Injection volume	1µL
	Split	1:50

Appendix 2: A total overview of the parameter settings applied during GCxGC method development. Parameter settings that were investigated and optimized are highlighted in green.

Process	Parameter	Setting
GCxGC	1D column	BPX5 20 m, 0.18 mm I.D., 0.18 µm D _f , 5% phenyl polysilphenylene-siloxane
	2D column	BPX50 5 m, 0.25 mm I.D., 0.25 µm D _f , 50% phenyl polysilphenylene-siloxane
	Transfer temperature	300°C
	Carrier gas	Helium
	Flow rate ¹ D	0.525 mL/min
	Flow rate ² D	20 mL/min
	Loop fill time	4.29 sec
	Loop flush time	225 msec
	Loop volume	50 µL
Oven	Oven initial temperature	40°C
	Oven temperature ramp	4.5 °C/min
	Oven end temperature	300°C
	Run time	64 min
MS	Mass range	29-450 amu
	Acquisition rate	4.4 Hz
FID	Acquisition rate	200 Hz
Liquid injection	Injection volume	1µL
	Split	1:50

Appendix 3: An overview of the 1D and 2D flow rate combinations applied for the determination of the operating window for GCxGC. Flow settings used for example calculations of loop fill time and loop flush time are highlighted in green.

1D flow rate (mL/min)	2D flow rate (mL/min)	Loop fill time (sec)	Loop flush time (msec)	Oven temperature ramp (°C/min)
0.4	15	5.63	300	3 & 6
0.4	17.5	5.63	257	6
0.4	20	5.63	225	6
0.4	22.5	5.63	200	6
0.4	25	5.63	180	3 & 6
0.45	15	5.00	300	6
0.45	17.5	5.00	257	6
0.45	20	5.00	225	6
0.45	22.5	5.00	200	6
0.45	25	5.00	180	6
0.45	27.5	5.00	164	6
0.5	15	4.50	300	6
0.5	17.5	4.50	257	6
0.5	20	4.50	225	3 & 6
0.5	22.5	4.50	200	6
0.5	25	4.50	180	6
0.5	27.5	4.50	164	6
0.55	15	4.09	300	6
0.55	17.5	4.09	257	6
0.55	20	4.09	225	6
0.55	22.5	4.09	200	6
0.55	25	4.09	180	6
0.55	27.5	4.09	164	6
0.6	15	3.75	300	3 & 6
0.6	17.5	3.75	257	6
0.6	20	3.75	225	6
0.6	22.5	3.75	200	6
0.6	25	3.75	180	3 & 6
0.6	27.5	3.75	164	6
0.65	15	3.46	300	6
0.65	17.5	3.46	257	6
0.65	20	3.46	225	6
0.65	22.5	3.46	200	6
0.65	25	3.46	180	6
0.65	27.5	3.46	164	6



Appendix 4: Example calculations for loop fill time and loop flush time. The calculations are based on a 1D flow rate of 0.4 mL/min and a 2D flow rate of 20 mL/min (appendix 3, highlighted in green). Loop volume was 50 μ L.

Loop fill time

Equation 1.
$$t_{75\% \text{ loop fill}} = \frac{V_{\text{loop}} \cdot 60}{1000 \cdot Q_{1D}} \cdot 0.75$$

$t_{75\% \text{ loop fill}}$ = Time needed to fill sample loop for 75% (sec)

V_{loop} = Loop volume (μ L)

60 = Conversion factor minutes to seconds

1000 = Conversion factor mL to μ L

Q_{1D} = 1st dimensional flow rate (mL/min)

0.75 = Fraction of loop filled

$$t_{75\% \text{ loop fill}} = \frac{50 \cdot 60}{1000 \cdot 0.4} \cdot 0.75 = 5.63 \text{ sec}$$

Loop flush time

Equation 2.
$$t_{150\% \text{ loop flush}} = \frac{V_{\text{loop}} \cdot 60000}{1000 \cdot Q_{2D}} \cdot 1.50$$

$t_{150\% \text{ loop flush}}$ = Time needed to flush sample loop for 150% (msec)

V_{loop} = Loop volume (μ L)

60000 = Conversion factor minutes to milliseconds

Q_{2D} = 1st dimensional flow rate (mL/min)

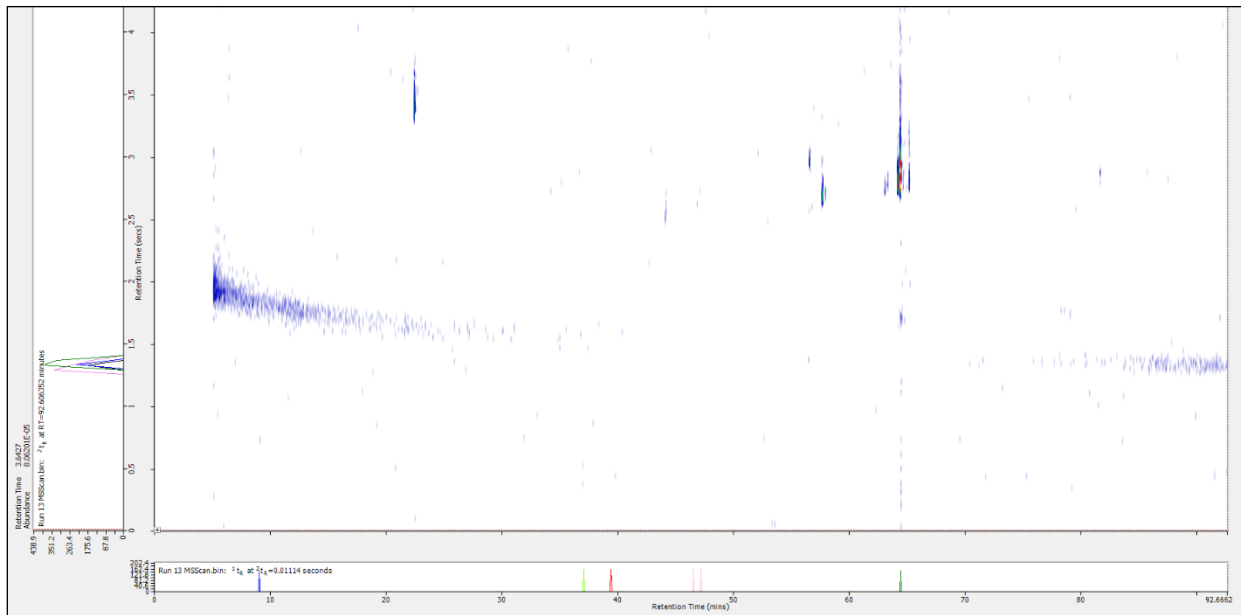
1.50 = Fraction of loop flushed

$$t_{150\% \text{ loop flush}} = \frac{50 \cdot 60000}{1000 \cdot 20} \cdot 1.50 = 225 \text{ msec}$$

Appendix 5: Peak height (counts) and peak area (counts•min) for p-xylene resulting from the corresponding 1D/2D flow rate combinations. The data was used to define the DoE factor ranges.

1D flow (mL/min)	Flow 2D mL/min	Peak area p-xylene (counts•min)	Peak height p-xylene (counts)
0.4	17.5	216178	47160
0.45	17.5	548493	192142
0.5	20	604245	202389
0.55	22.5	461148	139392
0.6	25	339915	74650
0.65	27.5	174489	38125

Appendix 6: The chromatogram acquired after GCxGC/MS analysis of DAA 1 with 1D flow rate 0.5 mL/min and 2D flow rate 20 mL/min. Oven temperature ramp was 3°C/min. Loop fill times and loop flush times were set at 75% and 150%, respectively. General parameter settings for liquid injection-GCxGC/MS are listed in white in appendix 2.



Appendix 7: An overview of 1D- and 2D flow rates (mL/min) and oven temperature ramps (°C/min) applied during the analyses of the DoE. The resulting peak areas for component C (counts•min), 2D retention times (sec) for components A and C, and 1D retention times (min) for components C and D are listed as well.

Nr.	1D flow (mL/min)	2D flow (mL/min)	Oven ramp (°C/min)	Area C (Counts•min)	RT 2D A (sec)	RT 1D C (min)	RT 2D C (sec)	RT 1D D (min)
1	0.475	19	3	120363	1.7505	64.509	2.8895	65.2876
2	0.475	19	4.5	262754	1.6499	46.6627	2.3446	47.1577
3	0.475	19	6	307410	1.5986	37.1200	2.0434	37.5536
4	0.475	20	3	108660	1.6399	66.6888	2.5258	67.5083
5	0.475	20	4.5	150070	1.5831	48.2302	2.1239	48.7335
6	0.475	20	6	131459	1.5364	38.4846	1.8967	38.9152
7	0.475	21	3	56183	1.5577	69.2976	2.2158	70.1488
8	0.475	21	4.5	58020	1.4950	50.2448	1.8678	50.8754
9	0.475	21	6	78060	1.4746	40.2758	1.7007	40.7737
10	0.5	19	3	213006	1.7692	62.7814	3.1448	63.5679
11	0.5	19	4.5	300520	1.6953	45.2223	2.5576	45.7252
12	0.5	19	6	354781	1.6309	35.9759	2.2586	36.3353
13	0.5	20	3	111527	1.6999	64.3578	2.8347	65.1459
14	0.5	20	4.5	149566	1.6047	46.4389	2.3316	46.9419
15	0.5	20	6	175667	1.5715	36.9809	2.0607	37.4069
16	0.5	21	3	79287	1.6110	66.2750	2.5094	67.0769
17	0.5	21	4.5	81656	1.5370	47.8750	2.0767	48.4478
18	0.5	21	6	94907	1.5006	38.1970	1.8657	38.6282
19	0.525	19	3	170576	1.8376	61.3454	3.4272	62.1349
20	0.525	19	4.5	194054	1.7152	44.1470	2.7479	44.6485
21	0.525	19	6	370118	1.6637	35.0433	2.3804	35.4750
22	0.525	20	3	155056	1.7451	62.6363	3.0843	63.4257
23	0.525	20	4.5	205117	1.6426	45.0776	2.4618	45.6515
24	0.525	20	6	262248	1.5852	35.8551	2.1827	36.2629
25	0.525	21	3	105994	1.6390	64.1438	2.7845	64.9298
26	0.525	21	4.5	125933	1.5844	46.2281	2.2362	46.7992
27	0.525	21	6	154854	1.5205	36.8366	2.0258	37.2665

Appendix 8: The table below can be seen as an extension of appendix 7 in terms of columns. Listed are peak widths at halve height in 2D for components A and C (sec), peak widths at halve height in 1D for components C and D, 1D resolution between C and D, and 2D resolution between A and C.

Nr.	W _{0.5h} 2D A (sec)	W _{0.5h} 1D C (min)	W _{0.5h} 2D C (sec)	W _{0.5h} 1D D (min)	Resolution CD 1D	Resolution AC 2D
1	0.0764	0.1036	0.1306	0.0925	4.6851	6.4929
2	0.0347	0.1347	0.1420	0.0877	2.6263	4.6392
3	0.0364	0.1114	0.1064	0.0846	2.6104	3.6755
4	0.0805	0.1486	0.1786	0.0952	3.9664	4.0346
5	0.0691	0.1849	0.1592	0.1105	2.0105	2.7952
6	0.0751	0.0993	0.1006	0.0863	2.7377	2.4198
7	0.0833	0.1453	0.1202	0.1340	3.5962	3.8160
8	0.0472	0.1620	0.1247	0.1139	2.6970	2.5591
9	0.0737	0.1187	0.1035	0.1355	2.3113	1.5056
10	0.1057	0.0953	0.1785	0.0908	4.9869	5.7115
11	0.0757	0.0944	0.1500	0.1004	3.0463	4.5083
12	0.0566	0.1009	0.1140	0.0871	2.2558	4.3417
13	0.0953	0.0992	0.1423	0.0817	5.1407	5.6358
14	0.0860	0.1684	0.1564	0.0858	2.3349	3.5385
15	0.0490	0.1931	0.1109	0.1290	1.5606	3.6101
16	0.0561	0.1419	0.1427	0.0922	4.0420	5.3326
17	0.0961	0.1032	0.1303	0.0873	3.5481	2.8129
18	0.0752	0.0994	0.1154	0.0894	2.6950	2.2603
19	0.1969	0.0949	0.1644	0.0923	4.9765	5.1916
20	0.0846	0.0929	0.1565	0.0822	3.3796	5.0543
21	0.1101	0.1003	0.1431	0.0831	2.7776	3.3401
22	0.1104	0.1071	0.1687	0.0909	4.7045	5.6620
23	0.0531	0.1418	0.1481	0.0857	2.9767	4.8045
24	0.0588	0.1926	0.1482	0.0831	1.7454	3.4060
25	0.0794	0.1309	0.1482	0.1273	3.5921	5.9389
26	0.0581	0.1340	0.1297	0.0867	3.0535	4.0954
27	0.0692	0.0931	0.1139	0.0848	2.8515	3.2564

Appendix 9: An example calculation for resolution. The calculation is based on the 2D RT of A and C, and on the 2D $W_{0.5h}$ of A and C resulting from analysis number two. The values as well as the resulting resolution are highlighted in green in appendix 7 and 8.

Equation 3:
$$R = 1.18 \cdot \left(\frac{RT_2 - RT_1}{W_{0.5h1} + W_{0.5h2}} \right)$$

R = resolution

RT = retention time (min)

$W_{0.5h}$ = peak width at half height (min)

2D resolution AC using equation 3

RT 2D A = 1.6499 sec

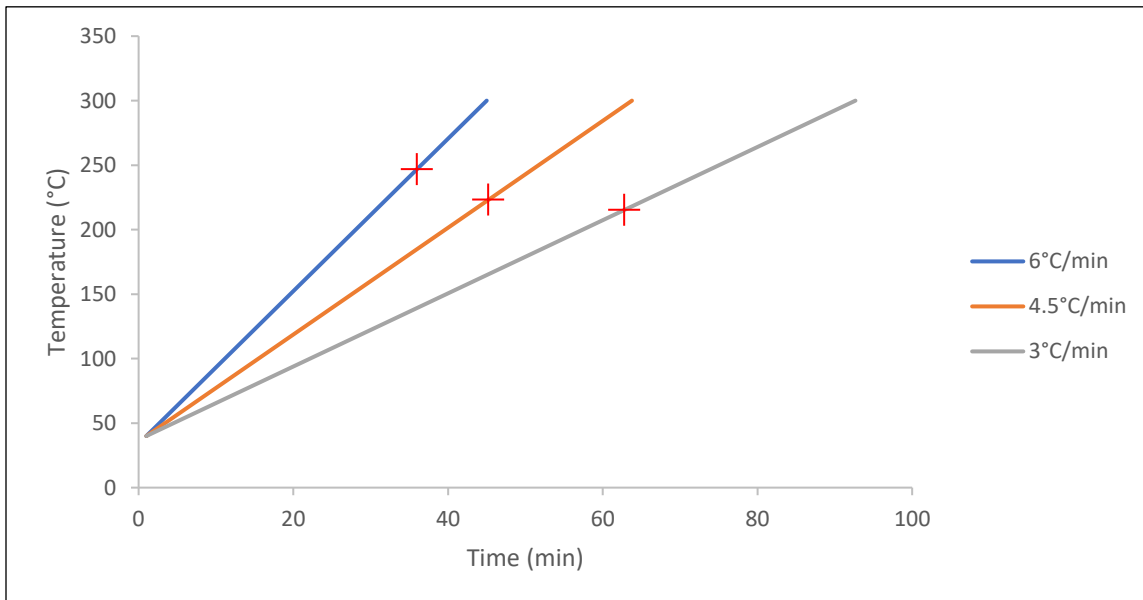
RT 2D C = 2.3446 sec

$W_{0.5h}$ 2D A = 0.0347 sec

$W_{0.5h}$ 2D C = 0.1420 sec

$$2D \text{ resolution AC} = 1.18 \cdot \left(\frac{2.3446 - 1.6499}{0.0347 + 0.1420} \right) = 4.6392$$

Appendix 10: Temperature (°C) vs time (min) for temperature ramps of 3, 4 and 6°C/min. Elution times for component C in DAA 1 are indicated with a red cross.



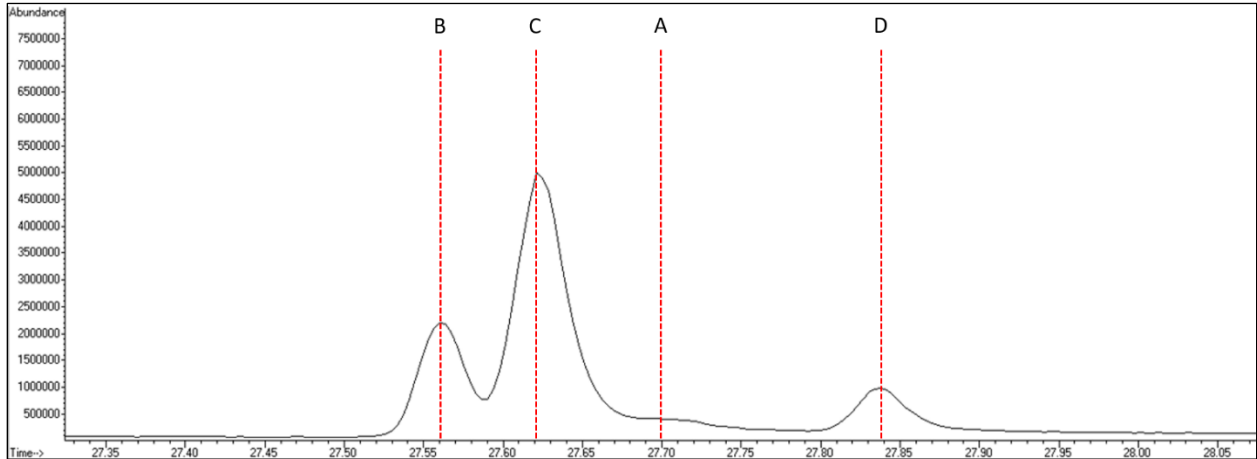
Appendix 11: Ten analyses were carried out with the developed GCxGC/MS method (appendix 2). Listed in the table below are first dimensional retention times (RT 1D) (min), second dimensional retention times (RT 2D) (sec) and peak areas for compound C (counts•min). Average values, standard deviations and RSDs are listed as well.

Analysis nr.	RT 1D C (min)	RT 2D C (sec)	Peak area C (counts•min)
1	37.094	2.056	479508
2	37.066	2.05	442372
3	37.070	2.056	343311
4	37.095	2.052	352946
5	37.032	2.059	406350
6	37.032	2.0338	401065
7	37.033	2.0578	367754
8	37.060	2.0491	338413
9	37.033	2.0317	391124
10	37.032	2.0585	340938
Average	37.055	2.050	386378
SD	0.026	0.010	47294
RSD (%)	0.070	0.503	12.2

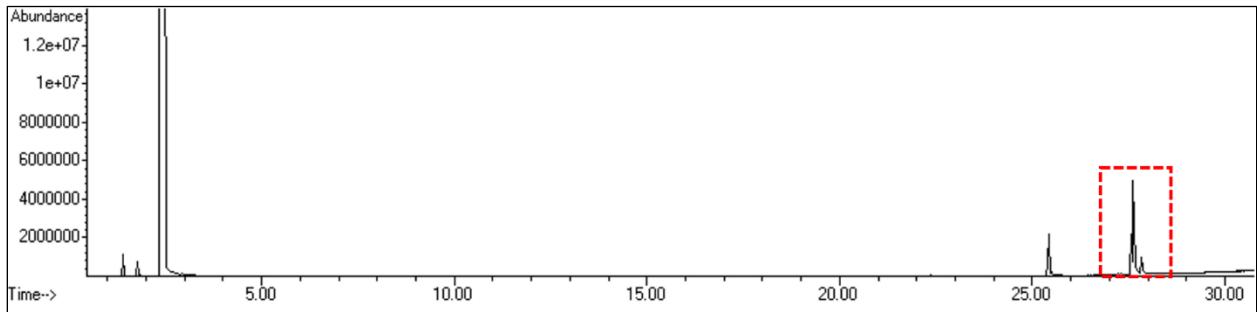
Appendix 12: Five analyses were carried out with the developed GCxGC method in combination with FID (appendix 2). Listed in the table below are the peak areas for compound C (counts•min). Average value, standard deviation and RSD are listed as well.

Analysis number	Area C (Counts•min)
1	44345700
2	44677500
3	44927600
4	44083300
5	43790100
Average	44364840
SD	453985
RSD (%)	1.023

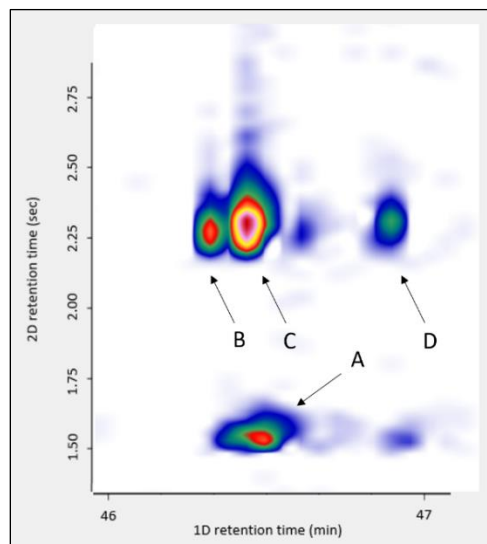
Appendix 13: A cut-out of the chromatogram resulting from single column GC/MS analysis of DAA 1. The applied parameter settings for liquid injection GC/MS are listed in appendix 1



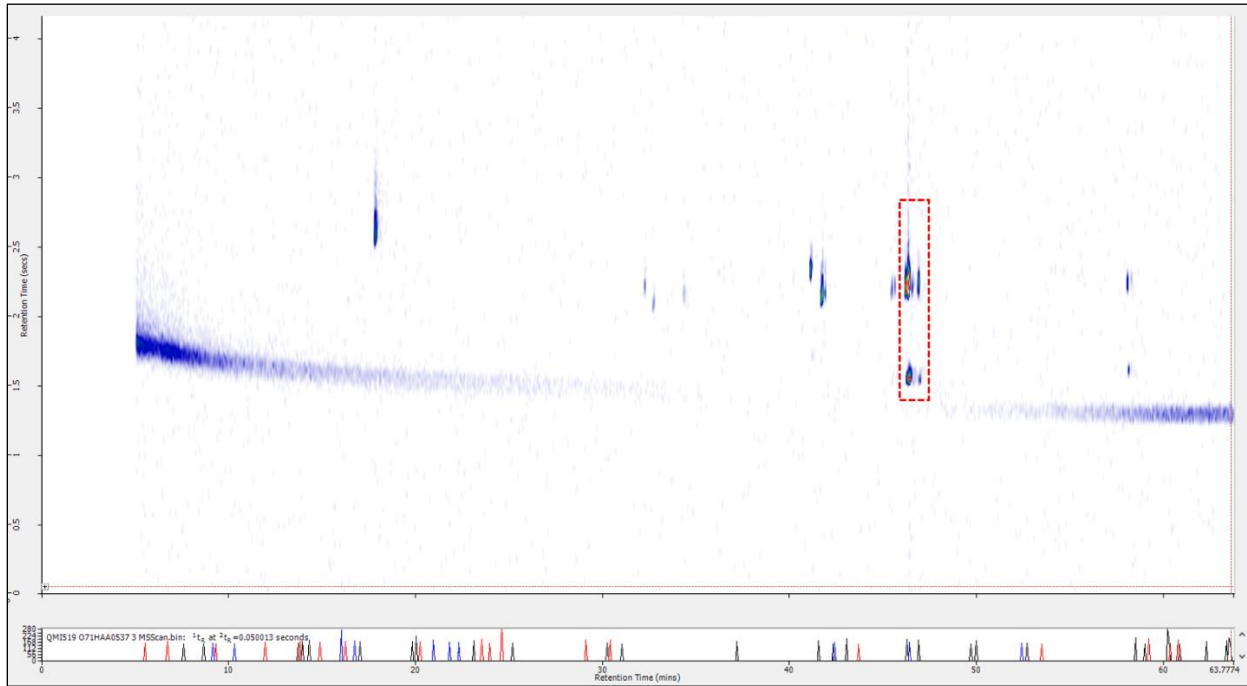
Appendix 14: The chromatogram resulting from single column GC/MS analysis of DAA 1. The applied parameter settings for liquid injection GC/MS are listed in appendix 1



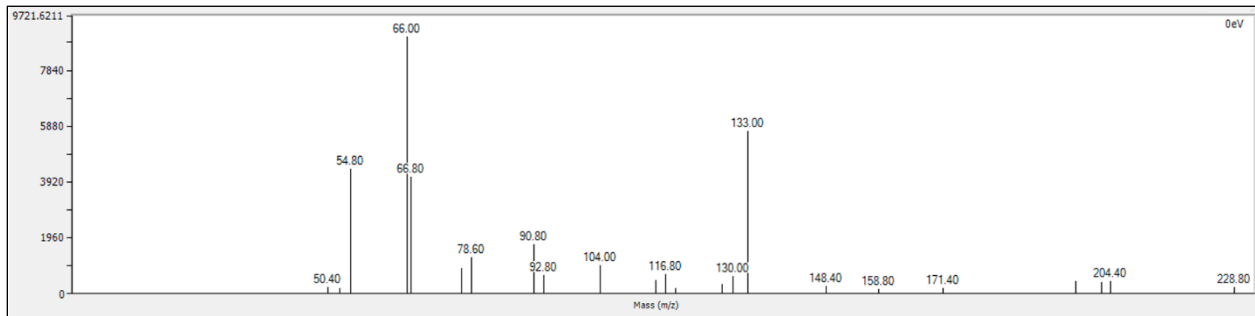
Appendix 15: The cut-out of the chromatogram resulting from GCxGC-MS analysis of DAA 1. The applied parameter settings for liquid injection GCxGC/MS are listed in appendix 2.



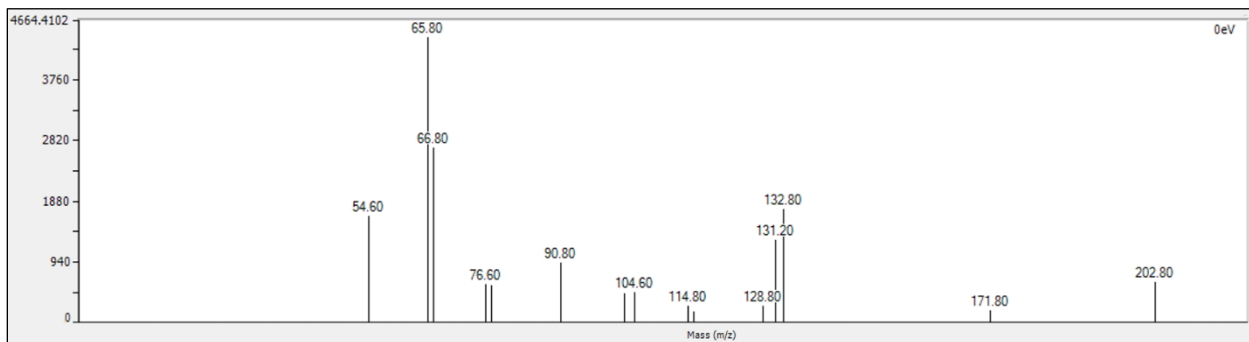
Appendix 16: Chromatogram resulting from GCxGC-MS analysis of DAA 1. The applied parameter settings for liquid injection GCxGC/MS are listed in appendix 2.



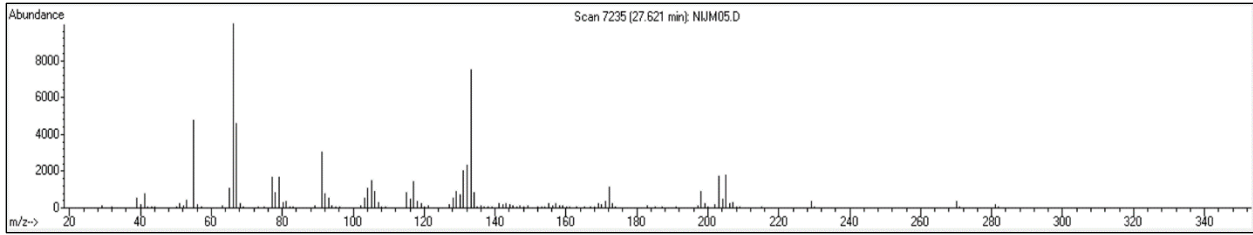
Appendix 17: MS spectrum of compound B after GCxGC/MS analysis of DAA 1. The applied parameter settings for liquid injection GCxGC/MS are listed in appendix 2.



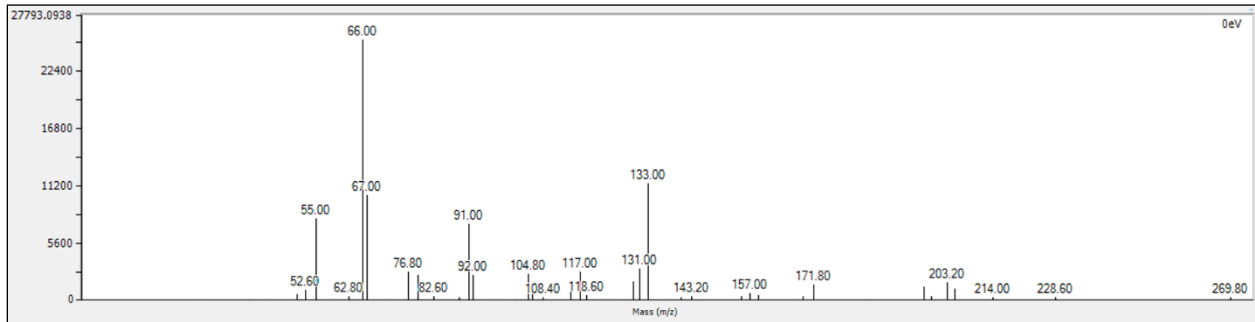
Appendix 18: MS spectrum of compound D after GCxGC/MS analysis of DAA 1. The applied parameter settings for liquid injection GCxGC/MS are listed in appendix 2.



Appendix 19: MS spectrum of compound C after single column GC/MS analysis of DAA 1. *The applied parameter settings for liquid injection GCxGC/MS are listed in appendix 1.*



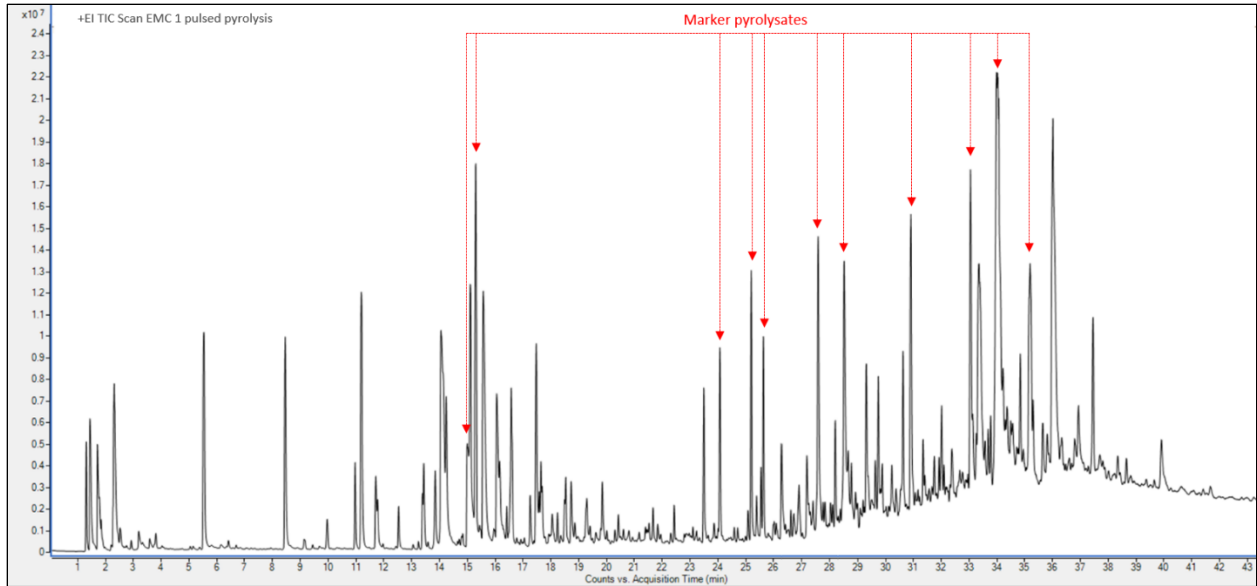
Appendix 20: MS spectrum compound C after GCxGC/MS analysis of DAA 1. *The applied parameter settings for liquid injection GCxGC/MS are listed in appendix 2.*



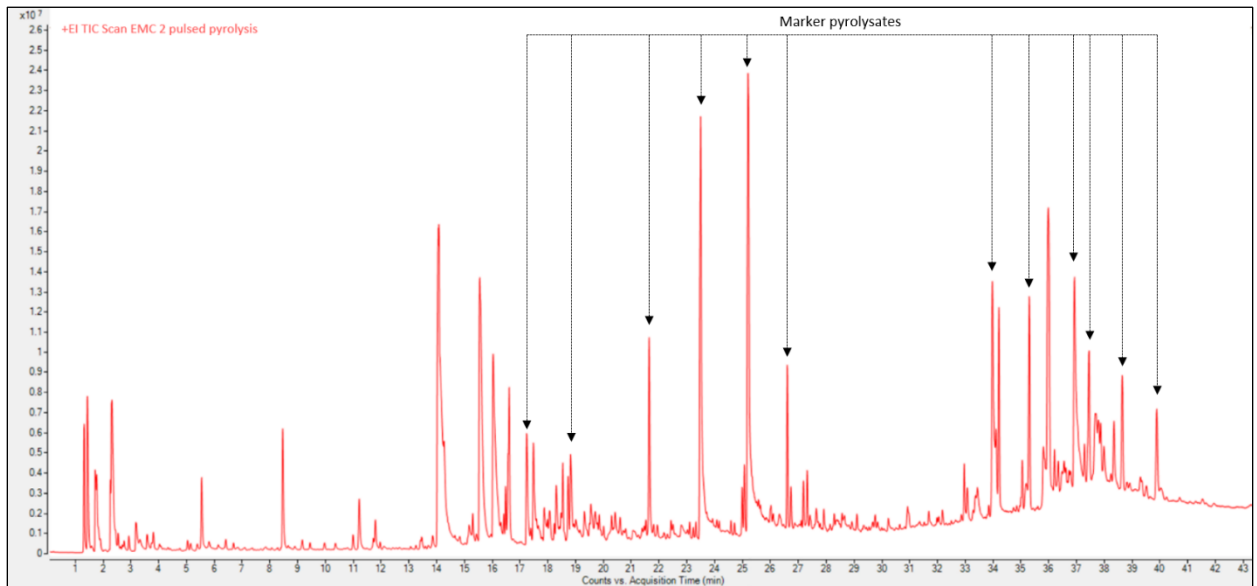
Appendix 21: An overview of parameter settings applied during PYR-GC/MS method development. Parameters that were selected during method development are highlighted in green.

Process	Parameter	Setting
Pulsed pyrolysis	TD initial temperature	40°C
	TD initial time	1.00 min
	TD temperature rate	60°C/min
	TD end temperature	280°C
	PYR initial temperatures	425°C & 575°C
	PYR temperature ramp	500°C/sec
	PYR initial time	12 sec
Smart ramp pyrolysis	TD initial temperature	70°C
	TD initial time	1.00 min
	TD temperature rate	5°C/min
	TD end temperature	350°C
	TD hold time	1.6 min
	PYR initial temperature	80°C
	PYR initial time	0.5 min
	PYR temperature ramp	5°C/sec
	PYR end temperature	625°C
	PYR initial time	12 sec
Oven	Initial temperature	40°C, 4 min hold
	Ramp 1	8°C/min to 300°C, 7 min hold
	Run time	43.5 min
GC/MS	Injector temperature	300°C
	Column	J&W VF-1ms, 30 m, 0.25 mm I.D., 1.00 µm D _f , 100% Dimethylpolysiloxane
	Carrier gas	Helium
	Flow rate	1.2 mL/min
	MS mass range	29-450 amu
CIS	Start temperature	-150°C
	Heating rate	12°C/sec
	End temperature	350°C, 5 min hold

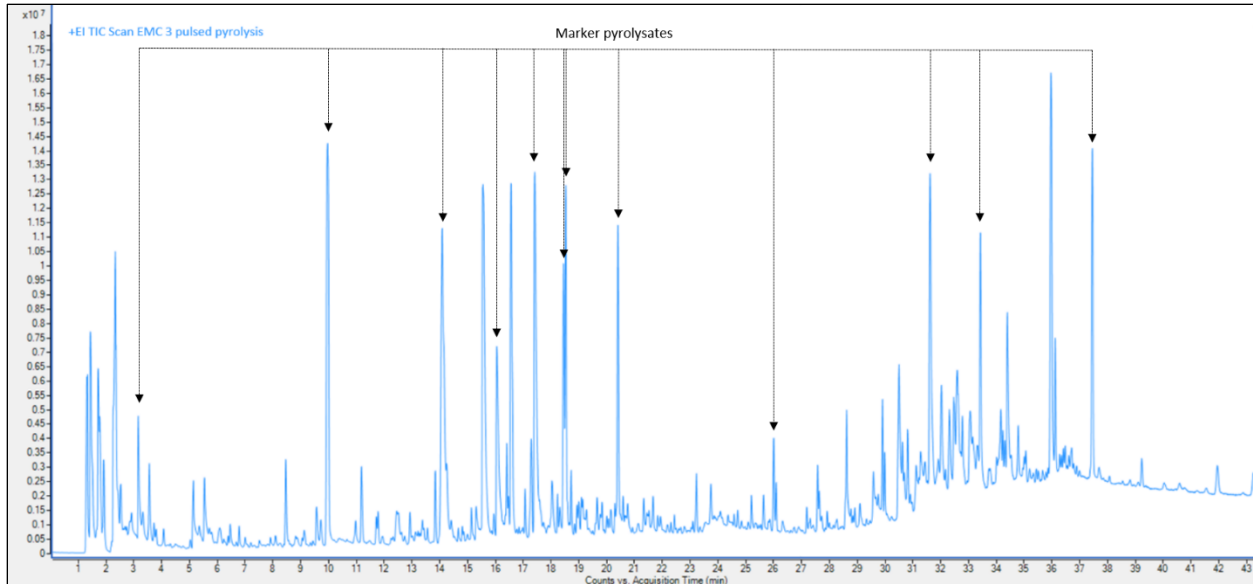
Appendix 22: The GC chromatogram resulting from pulsed PYR-GC/MS analysis of EMC 1. The applied parameter settings are listed in appendix 21. Marker pyrolysates are indicated by red arrows.



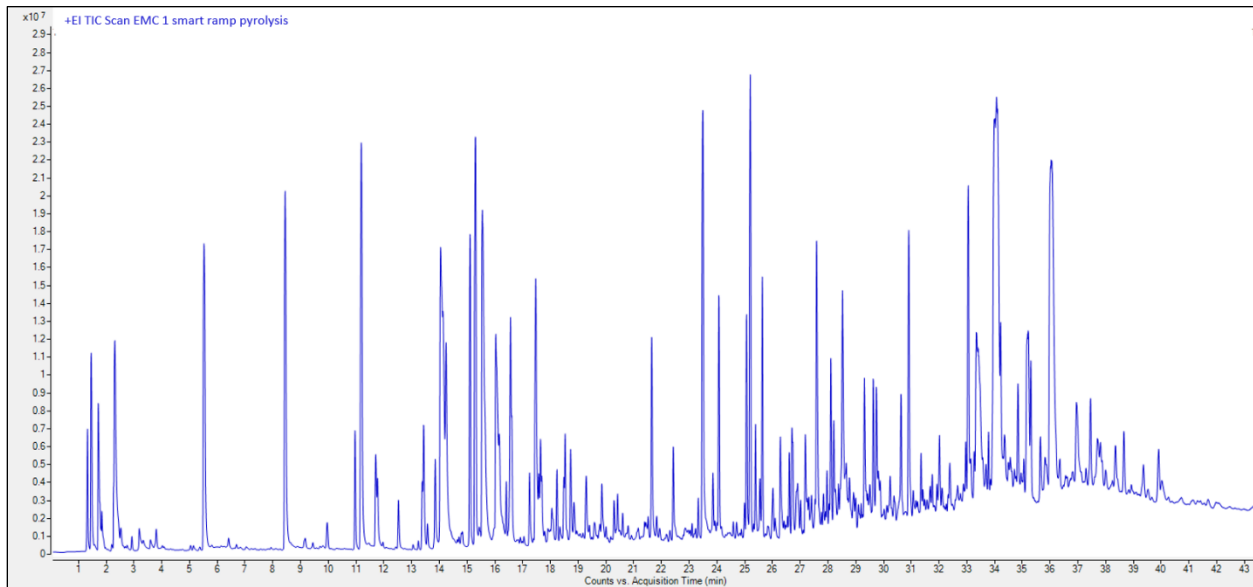
Appendix 23: The GC chromatogram resulting from pulsed PYR-GC/MS analysis of EMC 2. The applied parameter settings are listed in appendix 21. Marker pyrolysates are indicated by black arrows.



Appendix 24: GC chromatogram resulting from pulsed PYR-GC/MS analysis of EMC 3. The applied parameter settings are listed in appendix 21. Marker pyrolysates are indicated by black arrows.



Appendix 25: GC chromatogram resulting from smart ramp PYR-GC/MS analysis of EMC 1. The applied parameter settings are listed in appendix 21.



Appendix 26: Relative height of the twenty highest peaks with resulting RSD (%) found after triplo analysis of EMC1 with the developed PYR-GC/MS method (appendix 21). An overlay of the concerning chromatograms is illustrated in figure 28.

Nr.	Compound name	Fraction of greatest height (1 st)	Fraction of greatest height (2 nd)	Fraction of greatest height (3 rd)	RSD (%)
1	Propene	0.280	0.254	0.279	5.306
2	Acetone	0.602	0.598	0.629	2.830
3	Benzene	0.724	0.723	0.731	0.608
4	Toluene	0.677	0.654	0.672	1.792
5	Ethylbenzene	0.276	0.270	0.293	4.295
6	p-Xylene	0.631	0.607	0.616	1.981
7	Benzene, 1-ethyl-2-methyl-	0.267	0.252	0.280	5.277
8	Phenol	0.620	0.626	0.627	0.584
9	Indane	0.603	0.602	0.622	1.829
10	Indene	0.850	0.837	0.855	1.111
11	Phenol, 2-methyl-	0.456	0.456	0.460	0.428
12	Phenol, 3-methyl-	0.319	0.316	0.335	3.137
13	1,1'-Biphenyl, 3-methyl-	0.432	0.399	0.390	5.437
14	2,2'-Dimethylbiphenyl	0.323	0.326	0.343	3.318
15	Methane, di-p-tolyl-	0.297	0.369	0.356	11.177
16	Benzene, 1-methyl-2-(4-methylphenoxy)-	0.315	0.350	0.352	6.230
17	4,6,8-Trimethyl-1-azulenecarbaldehyde	0.271	0.326	0.322	10.063
18	2,6,2',6'-Tetramethyl-biphenyl-4,4'-diamine	0.652	0.692	0.685	3.113
19	4,4'-Dimethoxy-2,2'-dimethylbiphenyl	1.000	1.000	1.000	0.000
20	Triphenylphosphine oxide	0.942	0.930	0.792	9.372
				Average	3.89

Appendix 27: Retention times of the twenty highest peaks with resulting RSD (%) found after triplo analysis of EMC1 with the developed PYR-GC/MS method (appendix 21). An overlay of the concerning chromatograms is illustrated in figure 28.

Nr.	Compound name	RT 1 (min)	RT 2 (min)	RT 3 (min)	RSD (%)
1	Propene	1.444	1.438	1.438	0.241
2	Acetone	2.327	2.345	2.336	0.385
3	Benzene	5.538	5.551	5.543	0.118
4	Toluene	8.456	8.461	8.458	0.030
5	Ethylbenzene	10.968	10.969	10.968	0.005
6	p-Xylene	11.193	11.199	11.195	0.027
7	Benzene, 1-ethyl-2-methyl-	13.432	13.433	13.431	0.007
8	Phenol	14.075	14.075	14.072	0.012
9	Indane	15.106	15.106	15.106	0.000
10	Indene	15.298	15.299	15.299	0.004
11	Phenol, 2-methyl-	15.569	15.569	15.567	0.007
12	Phenol, 3-methyl-	16.056	16.057	16.055	0.006
13	1,1'-Biphenyl, 3-methyl-	23.491	23.49	23.489	0.004
14	2,2'-Dimethylbiphenyl	24.071	24.071	24.072	0.002
15	Methane, di-p-tolyl-	25.633	25.631	25.633	0.005
16	Benzene, 1-methyl-2-(4-methylphenoxy)-	27.59	27.589	27.586	0.008
17	4,6,8-Trimethyl-1-azulenecarbaldehyde	28.518	28.513	28.516	0.009
18	2,6,2',6'-Tetramethyl-biphenyl-4,4'-diamine	33.05	33.051	33.051	0.002
19	4,4'-Dimethoxy-2,2'-dimethylbiphenyl	34.014	34.021	34.015	0.011
20	Triphenylphosphine oxide	35.997	36.011	35.995	0.024
				Average	0.05